UNIVERSITY OF TURKU

The role of melanocortin 1 receptor in physiological cardiac hypertrophy in mice

Institute of Biomedicine
MDP in Biomedical Sciences, Drug Discovery and Development
Master's thesis

Author:
Aino Suni

Supervisors:
Docent Petteri Rinne
MSc Anni Suominen

21.03.2024
Turku

Master's thesis

Subject: Institute of Biomedicine, MDP in Biomedical Sciences, Drug Discovery and Development
Author(s): Aino Suni
Title: The role of melanocortin 1 receptor in physiological cardiac hypertrophy in mice
Supervisor(s): Docent Petteri Rinne, MSc Anni Suominen
Number of pages: 48 pages
Date: 21.03.2024

Melanocortin 1 receptor (MC1R) is known from its expression in the skin and regulation of skin and hair pigmentation. Recently, it has found to be expressed also in the heart, but its functional role has remained unknown. MC1R may have role in the regulation of cardiac hypertrophy, which is an adaptive response to increased cardiac workload due to exercise or cardiac disease. Exercise leads to physiological hypertrophy in which heart maintains or improves its function, whereas pathological hypertrophy occurs together with cardiovascular disease and leads to cardiac dysfunction and heart failure.

Here, we examined the potential involvement of cardiomyocyte-specific MC1R signaling in regulating of physiological cardiac hypertrophy. We subjected cardiomyocyte-specific MC1R knockout mice (Mc1r cKO) and their age-matched controls to voluntary wheel running to induce physiological cardiac hypertrophy and evaluated cardiac structure and function by echocardiography, histology, quantitative PCR and Western blotting.

We found that Mc1r cKO mice had lower left ventricular systolic function and increased left ventricular end-diastolic diameter compared to control mice after 5 weeks of voluntary wheel running, indicating attenuated response to exercise-induced cardiac remodeling. At the molecular level, we observed increased myosin heavy chain β (encoded by *Myh7* gene) expression in the heart of Mc1r cKO mice, which could explain the disturbance in cardiac remodeling. In conclusion, cardiac MC1R signaling is involved in the regulation of physiological cardiac hypertrophy. Findings of this study may have translational significance as *MC1R* has several dysfunctional variants in humans, which could be associated with an impairment in exercise-induced cardiac effects.

Key words: melanocortin 1 receptor, voluntary wheel running, physiological cardiac hypertrophy.

Table of contents

1 Introduction

1.1 Cardiac hypertrophy

The role of the heart is to pump blood to the circulatory system and ensure nutrient and oxygen supply for peripheral organs. Similarly, it pumps oxygen-poor blood back to the lungs. The heart is composed of cardiac myocytes along with various other cell types such as endothelial cells, vascular smooth muscle cells, fibroblasts, and cells of the immune system. Of these cells, cardiac myocytes play a pivotal role in facilitating heart's contractile function. Cardiac myocytes contain myofibril bundles, which consist of myofilaments and sarcomeres forming the fundamental contractile unit of the heart. (Bernardo et al., 2010.)

Different from the other cell types of the heart, cardiac myocytes have no ability to proliferate as they undergo terminal differentiation shortly after birth. In stressed conditions, the heart needs to preserve the blood flow of peripheral organs similarly as in a normal physiological state. This is achieved by raising stroke volume and heart rate, which increases the force to the myocardium. As response to this increased myocardial stress, cardiomyocytes enlarge and undergo a process named cardiac hypertrophy. Hypertrophy can be divided to physiological or pathological depending on the stimulus and underlying molecular mechanisms (Figure 1). Besides that, physiological and pathological cardiac hypertrophy differ in cardiac phenotype and prognosis. (Bernardo et al., 2010; Maillet et al., 2013; Mihl et al., 2008.)

In addition to classifying hypertrophy to physiological and pathological, it can be divided into concentric and eccentric cardiac hypertrophy based on heart morphology (Mihl et al., 2008; Weiner & Baggish, 2012). In concentric growth, there is an increase in both ventricular free wall and septal thickness, accompanied by a decrease in ventricular chamber dimension. Cardiomyocyte thickness is increased more than length. In eccentric growth, there is an increase in ventricular volume in addition to the thickening of ventricular wall and septum. Cardiomyocytes are longer and wider.

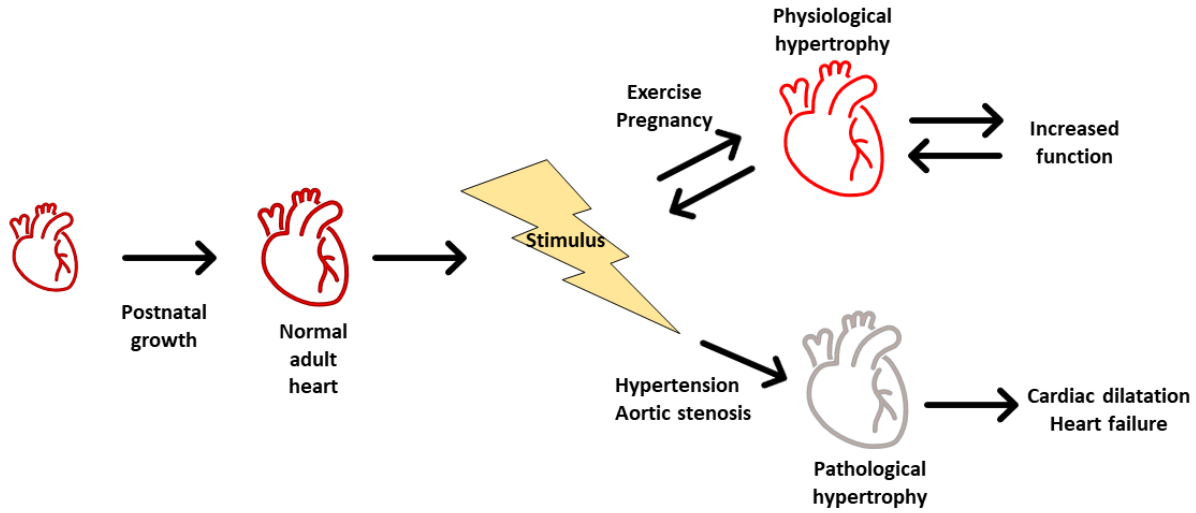

Figure 1. Cardiac hypertrophy means enlargement of cardiac myocytes as response to increased cardiac wall stress. Cardiac hypertrophy occurs as normal growth from birth to adulthood, as well as in response to different stimulus later in life. Depending on the type of stimulus, cardiac hypertrophy can be reversible or not and be classified to physiological and pathological, which differ in cardiac phenotype and prognosis.

1.1.1 Physiological hypertrophy

Physiological hypertrophy arises in response to increased workload during normal postnatal growth from birth to early adulthood, in the maternal heart during pregnancy, and in athletes as due to repetitive exercise (Maillet et al., 2013; Weiner & Baggish, 2012). Here, we focus on exercise-induced hypertrophy.

Exercise-induced cardiac hypertrophy is marked by a mild (10-20%) increase in cardiac mass, primarily caused by left-ventricle (LV) hypertrophy. The heart preserves or even increases its contractile function without any change in fibrosis or cell death. Physiological cardiac hypertrophy is completely reversible, meaning the cardiac changes begin to diminish after the stimulus is terminated. In addition, physiological hypertrophy does not progress into heart failure, and can even protect from it. (Bernardo et al., 2010.) Endurance training, which induces volume overload, leads typically to eccentric hypertrophy, while strength training, which induces pressure overload, leads to concentric hypertrophy (Baggish et al., 2008; Morganroth, 1975).

In physiological hypertrophy, cardiac structure and the pattern of cardiac gene expression are normal (Maillet et al., 2013; McMullen et al., 2003). Expression of fetal genes is not induced, and neither is the expression of fibrotic marker genes or proteins. Exercise training prevents unfavorable changes in sarcomere protein consistency, thus maintaining balanced myosin

heavy chain alpha ratio to myosin heavy chain beta (MHC-α/MHC-β ratio) (Rafalski et al., 2007). Exercise may even induce expression of MHC-α, which has higher ATPase activity and contractile velocity compared to MHC-β, and it therefore enhances the contractile function of the heart (Fernandes et al., 2015; Rafalski et al., 2007).

Furthermore, exercise enhanced the expression of peroxisome proliferator-activated receptor y co-activator 1a (PGC1a). PGC1a stimulates the production of vascular endothelial growth factor receptor, which in turn promotes angiogenesis. Additionally, exercise has been found to enhance endothelial nitric oxide synthase (eNOS) phosphorylation and relaxation of coronary arteries. Activation of PGC1a and eNOS enhance mitochondrial biogenesis. Mitochondria are responsible for substrate oxidation in cardiomyocytes, and in physiological hypertrophy, the metabolism between fatty acid and glucose oxidation is balanced. (Chen et al., 2022.)

Insulin-like growth factor 1 (IGF1) is one of the primary ligands activating the signaling pathway related to physiological cardiac hypertrophy (Maillet et al., 2013). Cardiac formation of IGF1 is increased and serum levels of IGF1 are elevated in athletes (Neri Serneri et al., 2001). IGF-1 binds to the IGF1 receptor, initiating the activation of phosphoinositide-3-kinases (PI3K) and downstream signaling molecule alpha serine/threonine-protein kinase (Akt). Akt is well known and essential for physiological heart growth as it activates regulatory proteins involved in protein synthesis and cell survival. IGF-1 has also direct positive inotropic effects (increase the force of heart contraction); it sensitizes myofilaments to Ca^{2+} or increases the availability of Ca^{2+} (Neri Serneri et al., 2001). In addition to these signaling molecules and pathways, extracellular signal-regulated kinases 1/2 (ERK1/2) and AMP-activated protein kinase (AMPK) are examples of signaling molecules having important roles in hypertrophic responses (Maillet et al., 2013).

1.1.2 Pathological hypertrophy

Pathological hypertrophy results from maladaptive reaction to increased workload in the presence of cardiovascular disease, such as myocardial infarction, hypertension or inflammatory myocardial disease (Mihl et al., 2008). These cardiovascular diseases cause pressure overload and an increase in cardiac wall stress mainly in the LV and left atrium. Right ventricular hypertrophy is usually caused by pulmonary arterial hypertension resulting from lung disease (Bernal-Ramirez et al., 2021). If the persistent increase in LV stress is not mitigated, it will lead to dilatation of the ventricle and cardiac dysfunction, which can ultimately

advance to heart failure (Bernardo et al., 2010). Heart failure presents a significant public health challenge and is one of the primary causes of death in Western countries.

At the molecular level, pathological cardiac hypertrophy is caused by changes in cardiac gene expression and alterations in molecular phenotype. Reactivation of fetal genes, which are not expressed in the normal adult heart, occurs in the hypertrophied heart, including upregulation of atrial natriuretic peptide (*Nppa*), brain natriuretic peptide (*Nppb*) and MHC-β (*Myh7*). Atrial natriuretic peptide (ANP) is secreted from cardiomyocytes in the atria and brain natriuretic peptide (BNP) from cardiomyocytes in the ventricles as a response to increased mechanical stretch (Epstein et al., 1998). ANP and BNP inhibit maladaptive cardiac hypertrophy by reducing vascular tone and by decreasing blood volume by inducing the production of urine. In addition, BNP has antifibrotic activity and is participating in the modulation of transforming growth factor β (*Tgfb1*) gene (Tamura et al., 2000). Additionally, ascended expression of MHC-β leads to a decreased MHC-α/MHC-β ratio, and further to nonfunctioning myosin molecule (Lyons et al., 1990; Weiss & Leinwand, 1996).

In addition to these changes, accumulation of extracellular matrix, increased fibrosis, inflammation induced by pro-inflammatory cytokines, as well as unfavorable changes in Ca^{2+} levels are characteristics of pathological hypertrophy. These factors will reduce the contractility of the heart and lead to cardiac dysfunction. Additionally, energy metabolism is switched from fatty acid oxidation to glycolysis. (Bernardo et al., 2010; Chen et al., 2022.)

In terms of involved signaling pathways, pathological stimulus leads to the formation of angiotensin II (Ang II), noradrenaline, and endothelin-1. These molecules activate G-protein coupled receptors (GPCR) and lead to dissociation of G_q, and subsequent activation of downstream signaling molecules resulting to pathological hypertrophy, fibrosis and inflammation (Bernardo et al., 2010). Ang II stimulates signaling molecules such as c-Jun amino-terminal kinases (JNKs), mitogen activated-protein kinases ERK1/2, and p38-MAP kinases and calcineurin. Further, Ang II enhances the formation of transforming growth factor-β leading to enhanced fibrosis (Lee et al., 1995; Nemoto et al., 1998).

Aging of population and increased prevalence of obesity have made heart failure more common in the past decades (Savarese et al., 2017). Furthermore, there is currently no cure for heart failure and underlying pathological hypertrophy (Bernardo et al., 2010). This is about to change since there is a rising interest in drug development for treating pathological hypertrophy as a

cause of heart failure. In addition, since exercise has protective effects against cardiovascular diseases (CVDs) including heart failure, in theory, exercise-like effects could be reached with pharmacological treatment if exact molecular mechanisms behind them are known, and utilized in treatment of CVDs (Chen et al., 2022; Gubert & Hannan, 2021).

1.2 Experimental models for physiological hypertrophy

To investigate physiological hypertrophy, different experimental models of exercise training have been developed and utilized. The most used experimental setups are swimming and running, and the most used animals in these setups are small rodents due to their low cost and short lifespan. Swine, dogs, and rabbits have also been used for exercise training protocols. Wildtype animals have been used to study basic physiology, whereas receptor knockout or overexpression models have been used to study the role of exact receptors on cardiac responses (Massett et al., 2021; Wang et al., 2010). Since there are several published protocols for exercise training, the comparison of the results can be somewhat difficult (Massett et al., 2021).

Forced treadmill running: In treadmill experiments, rodents are forced to run a certain time on a treadmill. Speed and inclination of treadmill can also be modified and controlled precisely, and the same training is applied to all animals (Kemi et al., 2002). Experiments last from weeks to months, and separate running sessions from minutes to hours.

Forced treadmill running is a well-controlled and an effective inducer of cardiac hypertrophy, especially in rats. It can increase heart/body weight ratio by up to 30% (Wang et al., 2010). In mice, the hypertrophy does not appear as strong as in rats (Kemi et al., 2002). Disadvantages of forced treadmill running are the need for special equipment and the stress caused to the animals. Stress reaction could elevate peripheral thyroid hormone levels, induce thymic involution and adrenal hypertrophy, while also reduce serum corticosteroid-binding globulin levels, and total adrenal medullary epinephrine contents (Wang et al., 2010).

Voluntary wheel running: In voluntary wheel running, animals have a running wheel in their home cage and can thereby determine the effort, frequency, and duration of exercise. The running pattern mirrors the natural running behavior of animals, and the running occurs under non-stressed conditions. No direct interference from the researcher is required, which further decreases the stress on animals. The amount of exercise can be automatically recorded. However, there might be overestimation of the amount of running results, because mice can roll the wheel without really running on it. It has been discovered that mice run spontaneously

4 to 20 km per day and maximal hypertrophy is seen after 3-4 weeks of running. (Manzanares et al., 2019.)

Swimming: In swim training, animals are placed into water tanks usually for 60 to 90 minutes per day for even 6 weeks (Kemi et al., 2002). The duration of the exercise can be precisely controlled, and many animals can be exercised simultaneously. Swim training results in a similar hypertrophic response compared to forced treadmill or voluntary wheel running (Wang et al., 2010). Water is not a natural environment for mice and therefore, causes additional stress for the animals. It has been found that water temperature changes the hypertrophic response depending on the animals' age (Prathima & Asha Devi, 1999).

Measurement of cardiac hypertrophy: Cardiac hypertrophy can be evaluated based on cardiac weight, size, and ventricular wall thickness (Basso et al., 2021). In addition, histological analysis can be performed to examine more closely the myocardium, including cardiomyocyte size, capillary network, and the presence of apoptosis. Together with basic hematoxylin and eosin (H&E) staining, connective tissue staining (such as Van Gieson, Masson's trichrome or PicroSirius red) and immunohistochemistry may be performed.

Since measurement of the heart weight does not reveal much about cardiac function, non-invasive imaging methods are needed. Echocardiography is a safe, widely available, and low-cost imaging method (Grant et al., 2021; Hillis & Bloomfield, 2005) to study cardiac structure and function. It enables longitudinal monitoring of changes in the heart, both before and after intervention. Commonly captured images include parasternal long-axis (PSLAX) and short-axis (SAX) views in two-dimensional brightness mode (B-mode) and motion mode (M-mode) images, along with pulsed-wave Doppler and tissue Doppler images (Grant et al., 2021).

In B-mode PSLAX imaging, the apex and base of LV is visualized on a same horizontal axis. On the contrary, in SAX view, cross-sectional images are obtained from the LV at different depths. B-mode imaging is used to assess chamber dimensions and cardiac structures such as valves and papillary muscles. In addition, functional parameters (cardiac output (CO), stroke volume (SV), fractional shortening (FS), ejection fraction (EF)), and estimation of LV mass can be calculated. B-mode imaging is a base for M-mode imaging, which shows the motion of myocardial wall over time in chosen single axis of B-mode scans. Left ventricular diameter during end-systole and end-diastole (LVESD and LVEDD), as well as SV, CO, EF and FS can be calculated based on M-mode imaging. (Lindsey et al., 2018; Moran et al., 2013.)

Doppler images are used to image moving targets, such as blood flow or myocardium. Pulse-wave doppler measures transvalvular flow-velocity, assessing diastolic function of the heart. Tissue Doppler measures myocardial velocities to assess left ventricular parameters of relaxation. (Lindsey et al., 2018; Moran et al., 2013.)

1.3 Melanocortin system

Melanocortins are a group of peptide hormones which undergo post-translational cleavage from the precursor molecule proopiomelanocortin (POMC). POMC production takes place in the pituitary gland in the brain, while its cleavage takes place both in the central nervous system (CNS) and in peripheral tissues. The cleavage results formation of α-, β-, and γ-melanocyte-stimulating hormones (α-, β-, and γ-MSH) and adrenocorticotropic hormone (ACTH) (Smith & Funder, 1988) (Figure 2). These endogenous melanocortins bind and activate melanocortin receptors MC1R, MC2R, MC3R, MC4R, and MC5R, all of which are G-protein coupled receptors (GPCR). (Cooray & Clark, 2011; Yang, 2011.)

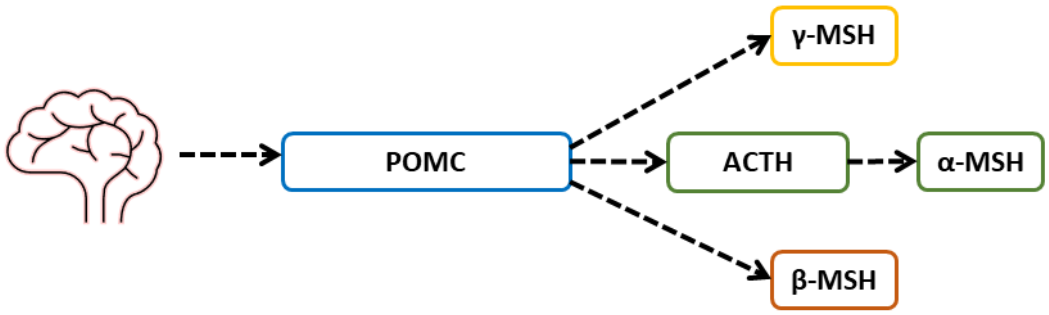

Figure 2. Overview of melanocortin hormones. Precursor molecule proopiomelanocortin (POMC) is produced in the pituitary gland in the brain, and it is cleaved to form α-, β-, and γ-melanocyte-stimulating hormones (α-, β-, and γ-MSH) and adrenocorticotropic hormone (ACTH).

Melanocortin receptors have varying tissue expressions and potencies for different melanocortin hormones. Furthermore, their physiological actions alter from receptor to receptor (Yang, 2011.). MC1R, found in melanocytes in the skin and hair follicles, is responsible for the synthesis of eumelanin and pigmentation of skin and hair (Wolf Horrell et al., 2016). MC1R is also expressed in leukocytes and macrophages, where it mediates anti-inflammatory effects. Moreover, MC1R is expressed in fibroblasts and endothelial cells. α-MSH is the main ligand for MC1R. (Catania et al., 2004.) A recent study revealed that MC1R is also abundantly expressed in the mouse heart (Thapa et al., 2023).

MC2R is expression is predominantly localized in the adrenal gland, where its activation promotes the expression of steroidogenic enzymes and steroid secretion (Cooray & Clark, 2011;

Mountjoy et al., 1992). Unlike other melanocortin receptor subtypes, MC2R is activated only by ACTH (Schiöth et al., 1996). MC3R is principally expressed in CNS and is activated equally by different melanocortins. The main roles of MC3R are in energy regulation and neural control of cardiovascular functions (Cooray & Clark, 2011; Versteeg et al., 1998). Similarly, MC4R is expressed in CNS and regulates intake of food, energy expenditure as well as sexual function and pain. MC5R is expressed in lymphocytes and exocrine glands, where it participates in the regulation of exocrine gland secretion (Cooray & Clark, 2011).

MCRs are coupled to stimulatory G_s-receptors, meaning that activation of MCRs leads to activation of adenylyl cyclase. This further increases the production of cyclic adenosine monophosphate (cAMP), which promotes activation of cAMP-dependent protein kinase A (PKA) and protein phosphorylation (Catania et al., 2004). For example, in melanocytes, activation of MC1R by α-MSH stimulates the formation of cAMP and subsequently induces activation of PKA, which finally leads to stimulation of melanogenesis (Buscà & Ballotti, 2000).

However, the same receptor can couple to different G proteins (including all types; G_s, $G_{i/o}$, G_q), and activate alternative signaling pathways and second messengers (Yang, 2011). In addition to activation of adenylyl cyclase, it has been shown that activation of MC1-MC5 receptors coupled to G_q or G_i protein by α-MSH increases intracellular calcium concentration as a second messenger (Kim et al., 1997; Mountjoy et al., 1992). Also, mitogen-activated protein kinases (MAPK) such as ERK1/2 are induced after melanocortin receptor activation. For example, MC3R activation stimulates the ERK1/2 pathway, which has an essential role in cell proliferation (Chai et al., 2007).

1.4 Melanocortins and cardiac remodelling

Melanocortin receptors are widely expressed in the CNS and peripheral organs, and it is known that they have a role in the central management of cardiovascular functions (Versteeg et al., 1998). Although α-MSH and at least MC1R, MC3R, and MC5R are expressed in the heart, their functional role has remained largely unexplored (Chhajlani, 1996; Thapa et al., 2023). There is clinical proof that circulatory levels of α-MSH are increased in heart failure patients, more in hypertrophic cardiomyopathy than in dilated cardiomyopathy (Yamaoka-Tojo et al., 2006). Pituitary gland could serve as a source for circulating α-MSH (Smith & Funder, 1988), but a hypertrophied heart might be also responsible for the production of α-MSH.

Research done in our group shows that α-MSH and POMC expression is upregulated in the mouse heart after transverse aortic constriction (TAC) -induced hypertrophy, while in the failing heart, the levels of α-MSH are declining. These findings suggest that the production of α-MSH is a protective mechanism against pathological cardiac hypertrophy. Later, it was proven that α-MSH mediates antihypertrophic effects in the heart by activating MC5R in cardiomyocytes (Suominen et al., 2023).

Subsequent studies in our group have demonstrated that MC1R is also expressed in the mouse heart and mediates opposite effects compared to MC5R. Specifically, we found that MC1R is abundantly expressed in cardiomyocytes and its expression is decreased after TAC-induced pressure overload. Additionally, mice with cardiomyocyte-specific deletion of MC1R showed blunted pathological hypertrophy after TAC surgery (unpublished data). Therefore it appears that MC1R and MC5R are counter-influencers of each other, *i.e.* activation of MC1R promotes pathological hypertrophy, while activation of MC5R activation protects from it.

The role of MC1R has also been examined in physiological cardiac hypertrophy. We have performed a voluntary running wheel experiment using mice that have a mutation in the *Mc1r* gene and are thus globally deficient in MC1R signaling ($Mc1r^{e/e}$, recessive yellow mice). The study revealed that $Mc1r^{e/e}$ mice had a blunted hypertrophic response to exercise compared to wildtype animals. In addition, in $Mc1r^{e/e}$ mice, EF did not increase as much as in wildtype animals after 5 weeks of voluntary wheel running (unpublished data). However, we do not know if this phenotype was specifically caused by dysfunctional MC1R in the heart or elsewhere in the body.

1.5 Aims and hypotheses

The purpose of this project is to examine the role of cardiac melanocortin 1 receptor in physiological cardiac hypertrophy. We hypothesize that cardiomyocyte-specific MC1R signaling is involved in the regulation of physiological cardiac hypertrophy. Since we know that global MC1R deficiency blunts exercise-induced physiological hypertrophy, we hypothesize that this phenotype is driven by MC1R signaling in cardiomyocytes and we aim to address this by utilizing cardiomyocyte-specific MC1R knockout (Mc1r cKO) mice. The specific aims of this study are:

1. To examine if Mc1r cKO mice show different heart weight, function, or cardiomyocyte histology compared to wildtype mice after 5 weeks of voluntary wheel running.

2. To examine if Mc1r cKO leads to different gene and protein expression of downstream signaling molecules and hypertrophic markers compared to wildtype mice after 5 weeks of voluntary wheel running.

2 Results

2.1 Body weight and running wheel data

Mice welfare was followed with weekly body weight measurements (Figure 3). There were no differences in body weight between the groups in the beginning of the experiment. Mice gained weight throughout the experiment, but a slight plateau was seen after tamoxifen dosing in weeks one and two in both sedentary and exercised groups (Figure 3).

At the end of the experiment (week 6), there was no statistical difference in body weight between sedentary and exercised control mice, meaning the development of weight was similar in control animals despite the exercising (Figure 3). At the same timepoint, body weight was significantly lower in exercised Mc1r cKO mice than in sedentary Mc1r cKO mice (P=0.014) (Figure 3).

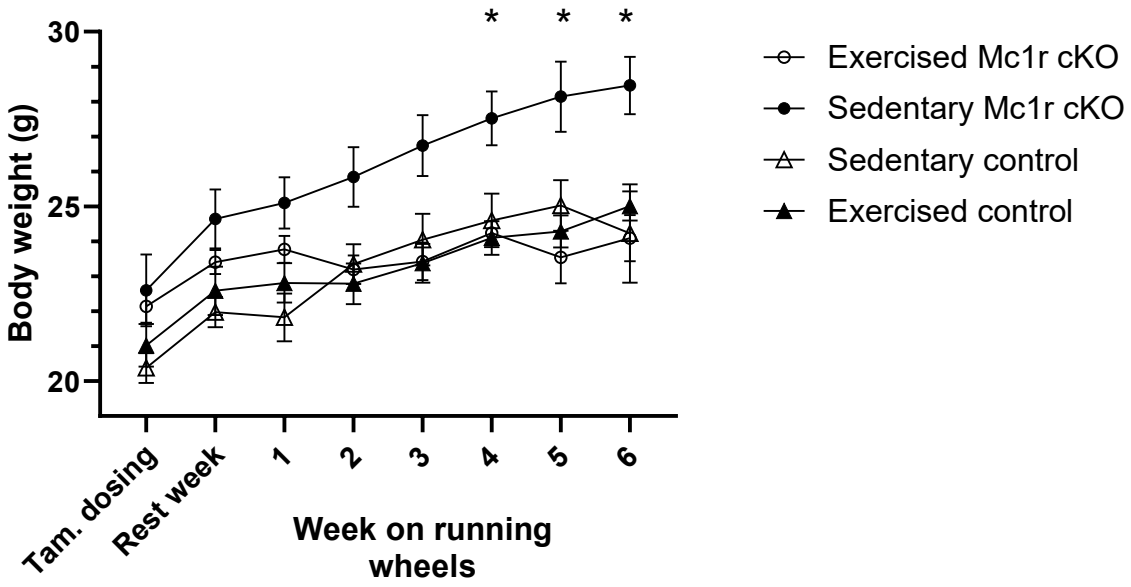

Figure 3. Body weight development during the experiment. Body weight was measured weekly throughout the experiment. n=11 in exercised Mc1r cKO mice, n=8 in exercised control mice, n=5 in sedentary Mc1r cKO mice and n=4 in sedentary control mice *P<0.05 sedentary Mc1r cKO compared to exercised Mc1r cKO. Mc1r cKO=cardiomyocyte-specific MC1R knockout. Tam. dosing = tamoxifen dosing. Running wheels were installed in the beginning of week 1. Values are mean ± SEM.

Voluntary wheel running was used to increase workload of the heart to induce physiological cardiac hypertrophy. Overall, the running pattern was similar between Mc1r cKO and control mice (Figure 4). Average total running distance during 5 week running experiment was 170 km in Mc1r cKO and 150 km in control mice without statistical difference between the groups (Figure 4A). However, there were major differences between individual mice as the highest

individual amount of running in Mc1r KO mice was 324 km and the lowest only 5 km whereas corresponding results in control mice were 236 km and 84 km.

Similarly, there were differences between individual mice in the highest running distance per 24h but no statistical differences between the genotypes in the average running distance per 24h (Figure 4B). After reaching the peak running distance per day during the third and fourth weeks of the experiment, the distance per day declined slightly towards the end of the experiment in both genotypes. Running activity was seen almost completely during the dark phase of the 12/12h light-dark cycle (between 19:00-7:00).

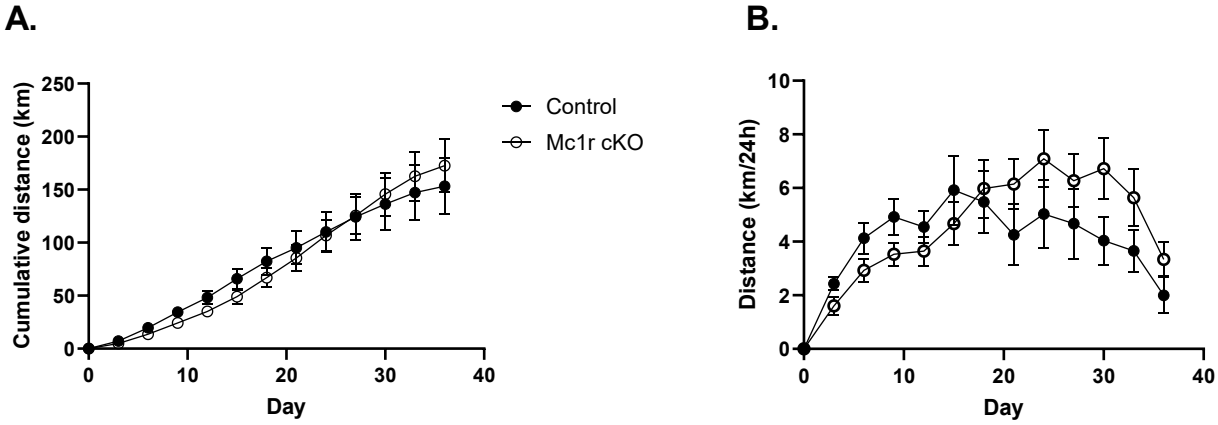

Figure 4. The amount of running was similar between genotypes in five-week voluntary wheel running experiment. A) Cumulative running distance in control and Mc1r cKO mice. B) Distance per day (km/24h) in control and Mc1r cKO mice. n=10 in Mc1r cKO mice, n=7 in control mice. Mc1r cKO=cardiomyocyte-specific MC1R knockout. Values are mean ± SEM.

2.2 Histological analysis and echocardiography imaging

First, absolute and relative venticular weight at sacrifice were measured to evaluate the effect of voluntary wheel running and cardiomyocyte-specific MC1R knockout on heart structure. The effect of exercise was not visible in absolute ventricular weight or ventricular weight relative to tibia length, but ventiruclar weight relative to bodyweight was higher in exercised mice compared to sedentary mice (P=0.0302 for the main effect of exercise from 2-way ANOVA) (Figure 5A-C).

After exercise ventricular weight relative to bodyweight was 9% higher in exercised Mc1r cKO mice compared to sedentary Mc1r cKO mice, and 14% higher in exercised control mice compared to sedentary control mice, which reflects higher increase in control mice heart weight compared to Mc1r cKO mice. In absolute ventricular weight difference was even more prominent, as exercised control mice had 14% higher ventriclular weight than sedentary control,

but in exercised Mc1r cKO mice ventricular weight was even 4% lower than in sedentary Mc1r cKO (Figure 5A).

Although there was not statistically significant difference between Mc1r cKO and control mice heart either in sedentary or exercised mice group, absolute ventricular weight (P=0.083) and ventricular weight normalized to tibia length (P=0.078) tended to be higher in sedentary Mc1r cKO compared to sedentary control mice (Figure 5A, 5C). In LV mass estimation from echogardiography analyses, difference was statistically significant, sedentary Mc1r cKO mice having higher LV mass compared to sedentary control mice (Figure 5D).

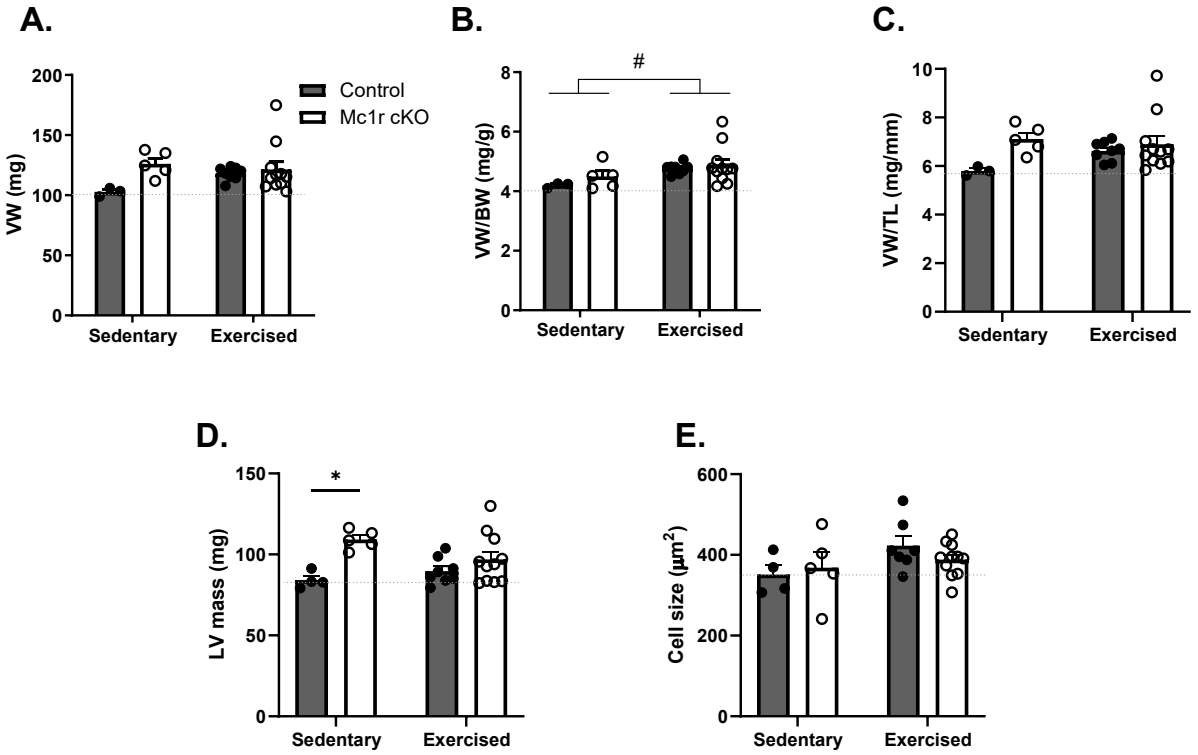

Figure 5. Relative heart weight increased after voluntary wheel running. A) Ventricular weight, B) ventricular weight/body weight, C) ventricular weight/tibia length (mg/mm), and D) left ventricular mass estimated by echocardiography imaging at the end of the experiment. E) Cardiomyocyte size quantified from hematoxylin and eosin (H&E) -stained sections. Data are mean ± SEM, each dot represent individual mouse. n=11 in exercised Mc1r cKO mice, n=8 in exercised control mice, n=5 in sedentary Mc1r cKO mice and n=4 in sedentary control mice. *P<0.05 for the indicated comparisons by 2-way ANOVA and Bonferroni's *post hoc* tests. #P<0.05, ##P<0.01 for the main effect of exercise by 2-way ANOVA. Mc1r cKO=cardiomyocyte-specific MC1R knockout, VW=Ventricular weight, BW=Bodyweight, TL=Tibia length, LV=Left ventricle.

Next, we wanted to see whether ventricular weight results are associated with changes in cardiomyocyte size. Measurement of the cross-sectional area of ventricular cardiomyocytes from H&E-stained sections indicated no statistically significant differences between any of the groups (Figure 5E). Exemplary H&E sections are presented in Figure 6.

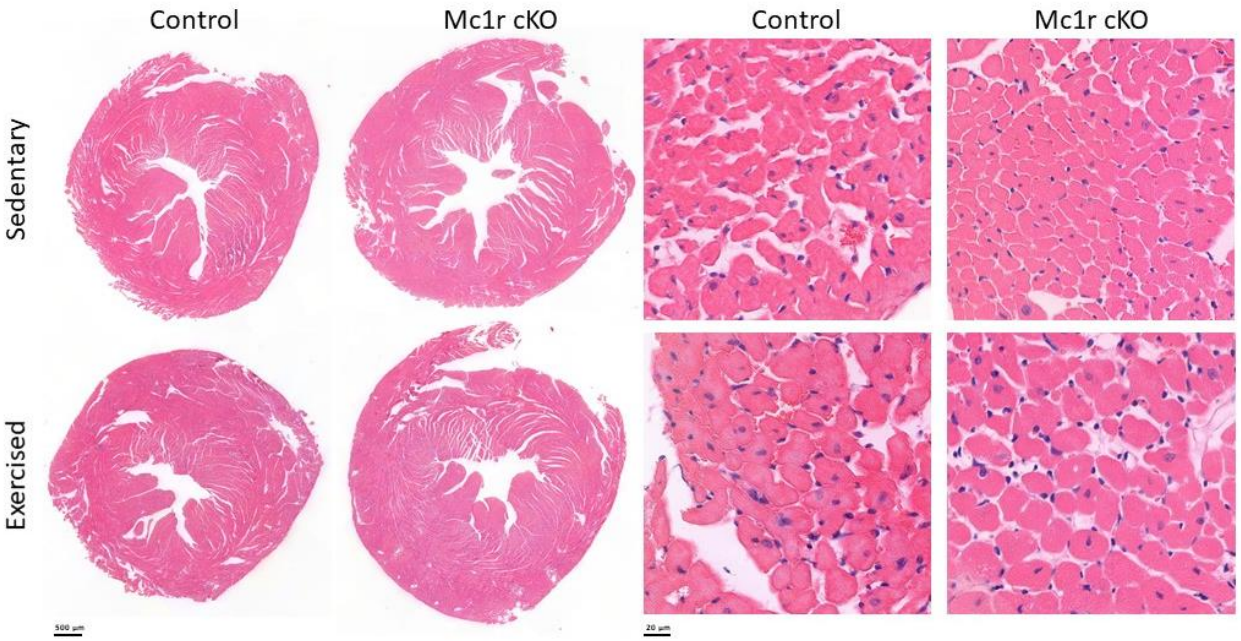

Figure 6. Representative cross sections of the heart stained with hematoxylin and eosin (H&E), illustrating the morphology and histology of the heart in the experimental groups. Scale bars: whole section 500 µm, myocyte section 20 µm. Mc1r cKO=cardiomyocyte-specific MC1R knockout.

To further investigate cardiac structure and function, we performed echocardiographic analyses. Echocardiography variables at the end of the experiment with or without the possibility of 5-week voluntary wheel running are presented in Figures 7 and 8. In exercised group, EF and FS were statistically significantly lower on Mc1r cKO mice compared to control mice (Figure 7A-B). On average, EF% was 12.50 and FS% was 9.20 lower in Mc1r cKO mice compared to control mice after 5-week exercising (Figure 7A-B).

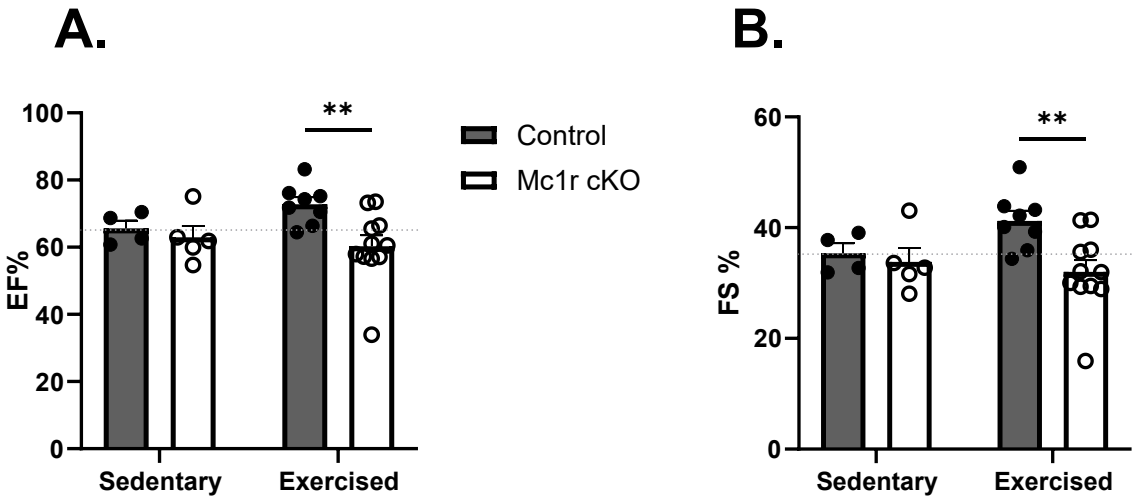

Figure 7. Cardiomyocyte-specific Mc1r knockout led to reduced LV systolic function after voluntary wheel running. A) Ejection fraction and B) fractional shortening analysed by echocardiography at the end of the experiment. Values are mean ± SEM, each dot represents individual mouse. N=11 in exercised Mc1r cKO mice, n=8 in exercised control mice, n=5 in sedentary Mc1r cKO mice and n=4 in

sedentary control mice. Mc1r cKO=cardiomyocyte-specific MC1R knockout. *P<0.05 and **P<0.01 for the indicated comparisons by 2-way ANOVA and Bonferroni's *post hoc* tests.

LVEDD was greater in Mc1r cKO mice compared to control mice in both sedentary and exercised group (Figure 8A). Similarly, LVESD was higher in exercised Mc1r cKO mice compared to control mice (Figure 8B). Relative wall thickness (RWT) was increased in exercised mice (P=0.0029 for the main effect of exercise from 2-way ANOVA), and was significantly lower in Mc1r cKO mice compared to control mice.

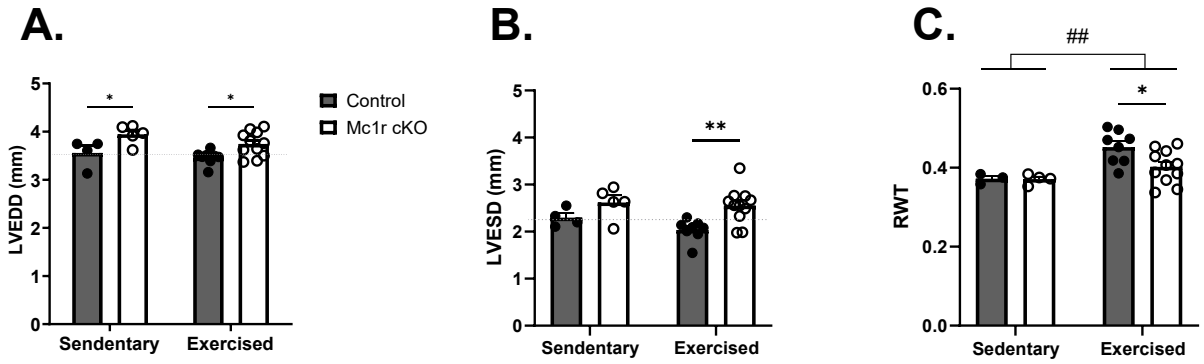

Figure 8. Cardiomyocyte-specific Mc1r knockout increased left ventricular diameter. A) Left ventricular end-diastolic diameter (LVEDD) and B) left ventricular end-systolic diameter (LVESD) at the end of the experiment. C) Relative wall thickness (RWT) at the end of the experiment. Values are mean ± SEM, each dot represents individual mouse. n=11 in exercised Mc1r cKO mice, n=8 in exercised control mice, n=5 in sedentary Mc1r cKO mice and n=4 in sedentary control mice. Mc1r cKO=cardiomyocyte-specific MC1R knockout. *P<0.05, **P<0.01 for the indicated comparisons by 2-way ANOVA and Bonferroni's *post hoc* tests. #P<0.05, ##P<0.01 for the main effect of exercise by 2-way ANOVA.

Exercising increased transmitral flow velocity ratio of early (passive) filling and late (active) filling (MV E/A) in both genotypes (P=0.0155 for the main effect of exercise by 2-way ANOVA) (Figure 9). MV E/A was significantly higher in exercised Mc1r cKO mice than in sedentary Mc1r cKO mice. Also, MV E/A tended to be higher in exercised Mc1r cKO mice compared to exercised control mice (P=0.0690).

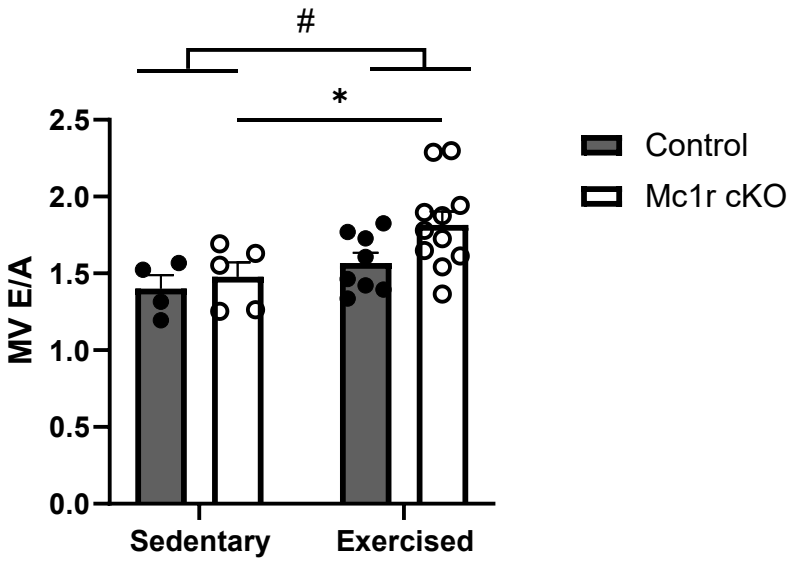

Figure 9. Voluntary wheel running increased MV E/A in Mc1r cKO mice. Transmitral flow velocity ratio of early (passive) filling and late (active) filling (MV E/A) analysed by pulsed wave Doppler echocardiography at the end of the experiment. Values are mean ± SEM, each dot represents individual mouse. n=11 in exercised Mc1r cKO mice, n=8 in exercised control mice, n=5 in sedentary Mc1r cKO mice and n=4 in sedentary control mice. Mc1r cKO=cardiomyocyte-specific MC1R knockout. *P<0.05 for the indicated comparisons by 2-way ANOVA and Bonferroni's *post hoc* tests. #P<0.05, ##P<0.01 for the main effect of exercise by 2-way ANOVA.

Next, to evaluate the genotype effect on exercise-induced cardiac hypertrophy and changes in LV systolic performance, we analyzed and compared echocardiography parameters at baseline and after 5-week voluntary running in control mice and Mc1r KO mice. Parameters describing LV systolic performance, EF and FS, tended to be lower in Mc1r KO mice already at baseline compared to control mice (EF P=0.2998, FS P=0.2193), but the difference became more appearent and significant after 5 weeks of running. This was due to the fact that EF and FS increased clearly in control mice (EF +6.4 % and FS +4.1 %), while Mc1r KO mice showed no effect in this regard (EF +1 % and FS +0.8 %) (Figure 10A-B).

Next, left ventricular posterior and anterior wall thicknessess (LVPW and LVAW) were measured to evaluate hypertrophic remodelling of the LV in response to voluntary wheel running. In the beginning of the experiment, LVPW thickness was slightly higher in Mc1r cKO mice compared to control mice (P=0.0822), but after exercising control mice reached the level of Mc1r cKO mice (P=0.8766) (Figure 10C). In LVAW, there was no difference between genotypes at the baseline but after exercising LVAW was significantly thinner in Mc1r cKO mice comprared to control mice. In addition, Mc1r cKO showed increased LVEDD and LVESD, whereas these parameters decreased in control mice in response to exercise. This led

to statistically significant difference in LVEDD and LVESD between genotypes at the end of the experiment (Figure 10E-F).

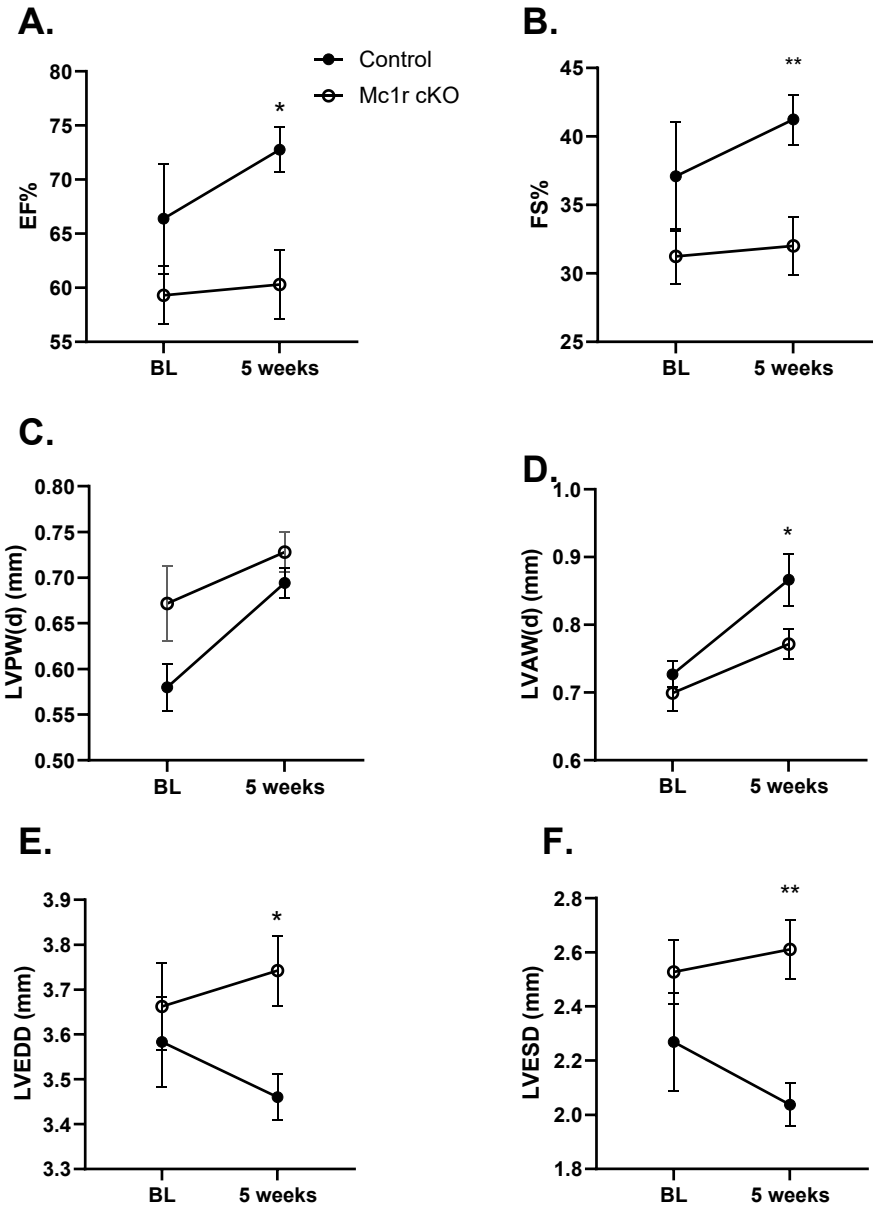

Figure 10. Cardiomyocyte specific Mc1r knockout led to lower LV systolic function and milder increase in LV wall thicknesses after voluntary wheel running. A) Ejection fraction, B) fractional shortening, C) LV posterior wall thickness during diastole, D) LV anterior wall thickness during diastole, E) LV end-diastolic diameter, and F) LV end-systolic diameter in exercised control and Mc1r cKO mice at baseline and after five weeks of wheel running. Values are mean ± SEM. Mc1r cKO n=11, control n=8. Mc1r cKO=cardiomyocyte-specific MC1R knockout. *P<0.05 and **P<0.01 for the indicated comparisons by 2-way ANOVA for repeated measures and Bonferroni's *post hoc* tests.

Other ultrasound parameters assessing systolic and diastolic function, measured at the end of the experiment, are reported in Table 1. However, the change in none of these parameters reached statistical significance.

Table 1. Results from cardiac ultrasound imaging performed at the 5-week time point.

Parameter	Sedentary		Exercised	
	Control	Mc1r cKO	Control	Mc1r cKO
SV	35.09 ± 3.73	42.26 ± 0.82	36.03 ± 1.27	35.81± 2.05
CO	13.73 ± 1.29	16.24 ± 0.82	13.96 ± 0.59	13.76 ± 0.96
IVRT (ms)	19.64 ± 2.12	22.34 ± 1.33	20.21 ± 1.67	17.91 ± 1.23
MV deceleration time (ms)	16.17 ± 1.58	24.11 ± 3.23	31.47± 5.51	22.08 ± 2.37
MV E/E'	54.15 ± 6.97	54.25 ± 8.26	31.19 ± 26.91	54.08± 12.04

SV=stroke volume, CO=cardiac output, IVRT=isovolumetric relaxation time, MV E/E' velocity divided by mitral annular E' velocity (=LVEDP). n=11 in exercised Mc1r cKO mice, n=8 in exercised control mice, n=5 in sedentary Mc1r cKO mice and n=4 in sedentary control mice. Mc1r cKO=cardiomyocyte-specific MC1R knockout. Values are presented as mean ±SEM.

2.3 Western blotting

To study possible signalling pathways involved in hypertrophic response induced by voluntary wheel running and differences in protein expression of hypertrophic markers between Mc1r cKO and control mice, we extracted total protein from LV samples and performed Western blotting analysis. We analysed expression of several MAPKs (phosphorylated and total protein) and hypertrophic marker proteins.

Exercise increased AKT and p38 pathway activation as evidenced by increase of phosphorylated forms of AKT (p-AKT) and p38 (p-p38) in exercised mice compared to sedentary mice (Figure 11A-B). In addition, there was a slight difference between genotypes in phosphorylated JNK (p-JNK) expression normalized with GAPDH (glyceraldehyde-3-phosphate-dehydrogenase), as p-JNK expression tented (P=0.1465) to be lower in exercised Mc1r cKO compared to exercised control mice (Figure 11C).

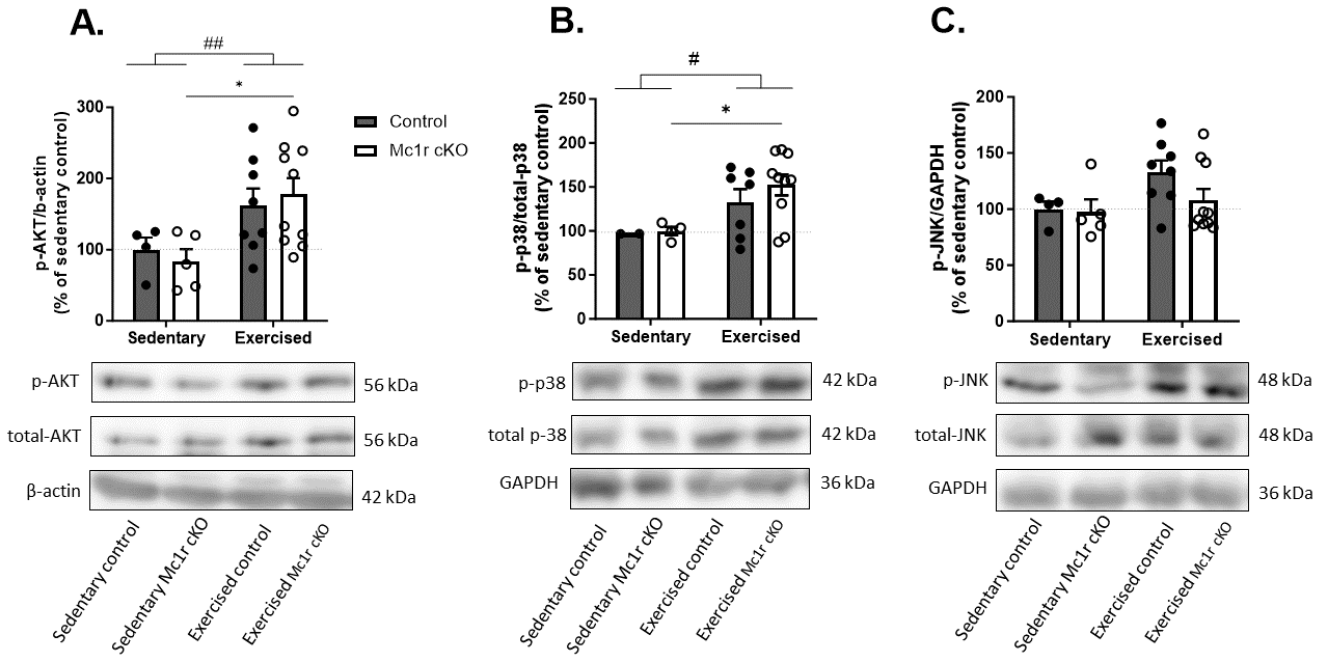

Figure 11. Voluntary wheel running increased p-AKT and p-p38 expression in the heart. Representative Western blots and quantification of A) p-AKT, B) p-p38, and C) p-JNK expression in LV samples . Data are mean ± SEM, each dot represents individual mouse. n=10 in exercised Mc1r cKO mice, n=8 in exercised control mice, n=5 in sedentary Mc1r cKO mice and n=4 in sedentary control mice. Mc1r cKO=cardiomyocyte-specific MC1R knockout. *P<0.05, **P<0.01 for the indicated comparisons by 2-way ANOVA and Bonferroni's *post hoc* tests. #P<0.05, ##P<0.01 for the main effect of exercise by 2-way ANOVA.

In addition, expression of other phosphorylated signalling proteins was studied (Figure 12). However, there were no statistically significant differences between the different groups in p-ERK, p-AMPK or p-CREB (cAMP-response element binding protein) expression.

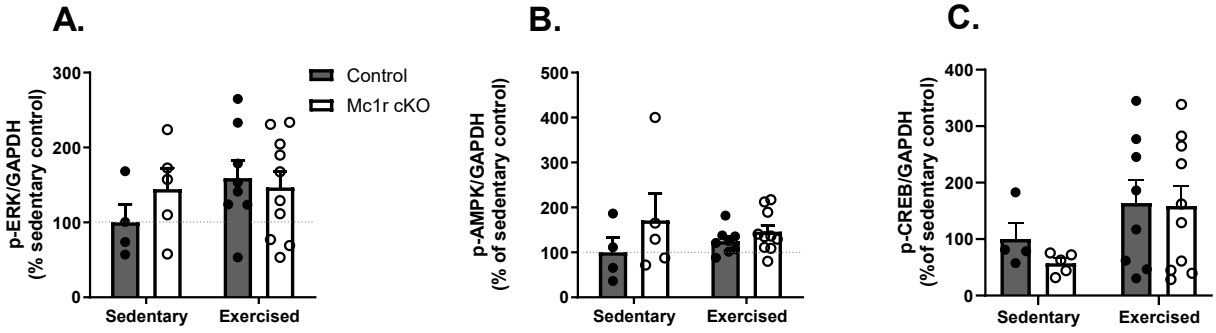

Figure 12. Phosphoprotein expression in cardiomyocyte-specific Mc1r knockout and control mice. A) p-ERK, B) p-AMPK, and) p-CREB expression in LV samples. Data are mean ± SEM, each dot represent individual mouse. n=10 in exercised Mc1r cKO mice, n=8 in exercised control mice, n=5 in sedentary Mc1r cKO mice and n=4 in sedentary control mice. Mc1r cKO=cardiomyocyte-specific MC1R knockout.

MC1R deficiency weakened exercise-induced hypertrophy evidenced by decreased BNP protein expression in Mc1r cKO mice compared to control mice after 5-week voluntary running

as well as compared to sedentary Mc1r cKO mice (P=0.0310 for the interaction between genotype and exercise by 2-way ANOVA) (Figure 13A). In exercised control mice BNP expression tended to increase compared to sedentary control mice (P=0.10). MHC-β expression was not statistically significantly altered by 5-week voluntary wheel running, but its expression was higher in Mc1r cKO mice compared to control mice (Figure 13B).

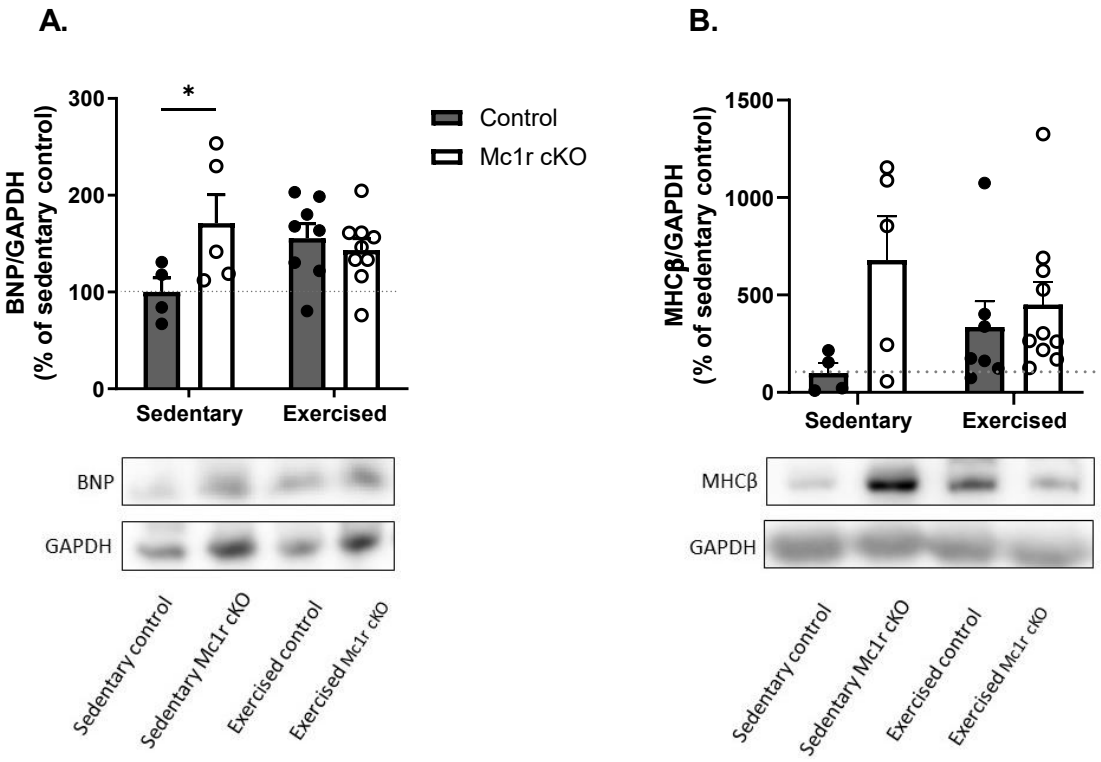

Figure 13. BNP expression was increased in sedentary Mc1r cKO mice. Representative Western blots and quantification of A) BNP, and B) MHCβ expressions in LV samples. Data are mean ± SEM, each dot represents individual mouse. n=10 in exercised Mc1r cKO mice, n=8 in exercised control mice, n=5 in sedentary Mc1r cKO mice and n=4 in sedentary control mice. Mc1r cKO=cardiomyocyte-specific MC1R knockout. *P<0.05 for the indicated comparisons by 2-way ANOVA and Bonferroni's *post hoc* tests.

PGC1a expression tended to increase in control mice as response to exercising (P=0.1117) (Figure 14).

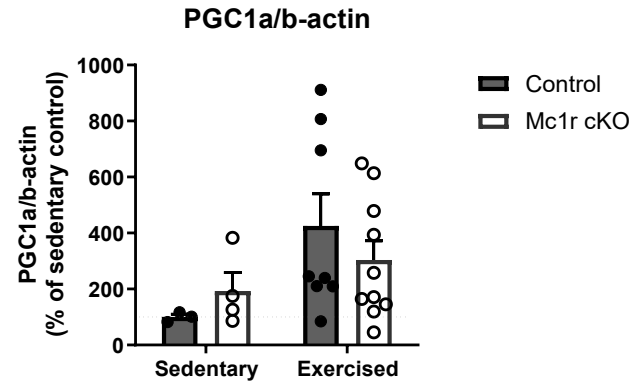

Figure 14. Quantification of PGC1a expression in LV samples of Mc1r cKO and control mice. Data are mean ± SEM, each dot represents individual mouse. n=10 in exercised Mc1r cKO mice, n=8 in exercised control mice, n=5 in sedentary Mc1r cKO mice and n=4 in sedentary control mice. Mc1r cKO=cardiomyocyte-specific MC1R knockout.

2.4 Gene expression analyses

To study changes in the gene expression of hypertrophic markers in the heart, we ran quantitative real time polymerase chain reaction (qRT-PCR) analysis from the LV samples. In addition, we were interested in cardiac lipid metabolism and analysed genes related to fatty acid oxidation and lipid transport.

Cardiac *Myh7* mRNA expression was higher in Mc1r cKO mice compared to control mice (P=0.0143 for the main effect of genotype by 2-way ANOVA), but difference was statistically significant only in exercised mice (Figure 15A). In terms of *Myh6* expression, there was no statistically significant differences between the groups (figure 15B). Consequently, *Myh6/Myh7* ratio was significantly lower in exercised Mc1r cKO compared to control mice (Figure 15C). Ratio tended to be lower also in sedentary Mc1r cKO mice compared to sedentary control mice (P=0.2195).

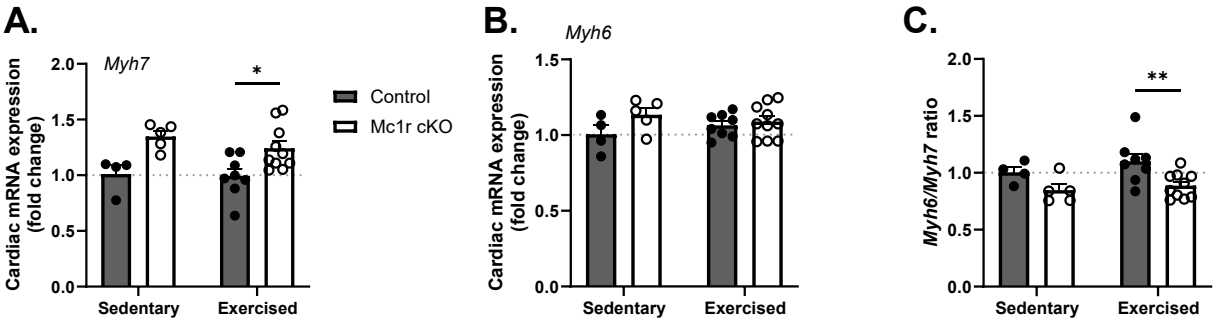

Figure 15. *Myh7* expression was increased in Mc1r cKO mice. A) *Myh7* (myosin heavy chain b) and B) *Myh6* (myosin heavy chain a) cardiac mRNA expressions. C) *Myh6/Myh7* (MHCα/MHCβ) ratio. Data are mean ± SEM, each dot represents individual mouse. n=10 in exercised Mc1r cKO mice, n=8 in exercised control mice, n=5 in sedentary Mc1r cKO mice and n=4 in sedentary control mice. Mc1r

cKO=cardiomyocyte-specific MC1R knockout. *P<0.05, **P<0.01 for the indicated comparisons by 2-way ANOVA and Bonferroni's *post hoc* tests.

Hypertrophic marker *Nppb* expression decreased due to exercise (P=0.0023 for the main effect of exercise by 2-way ANOVA), but the change was only statistically significant in Mc1r cKO mice (Figure 16A). *Nppa,* skeletal alpha actin *(Acta1)* and smooth muscle actin *(Acta2)* gene expressions were not altered by either the Mc1r cKO genotype or by exercise (Figure 16B-D).

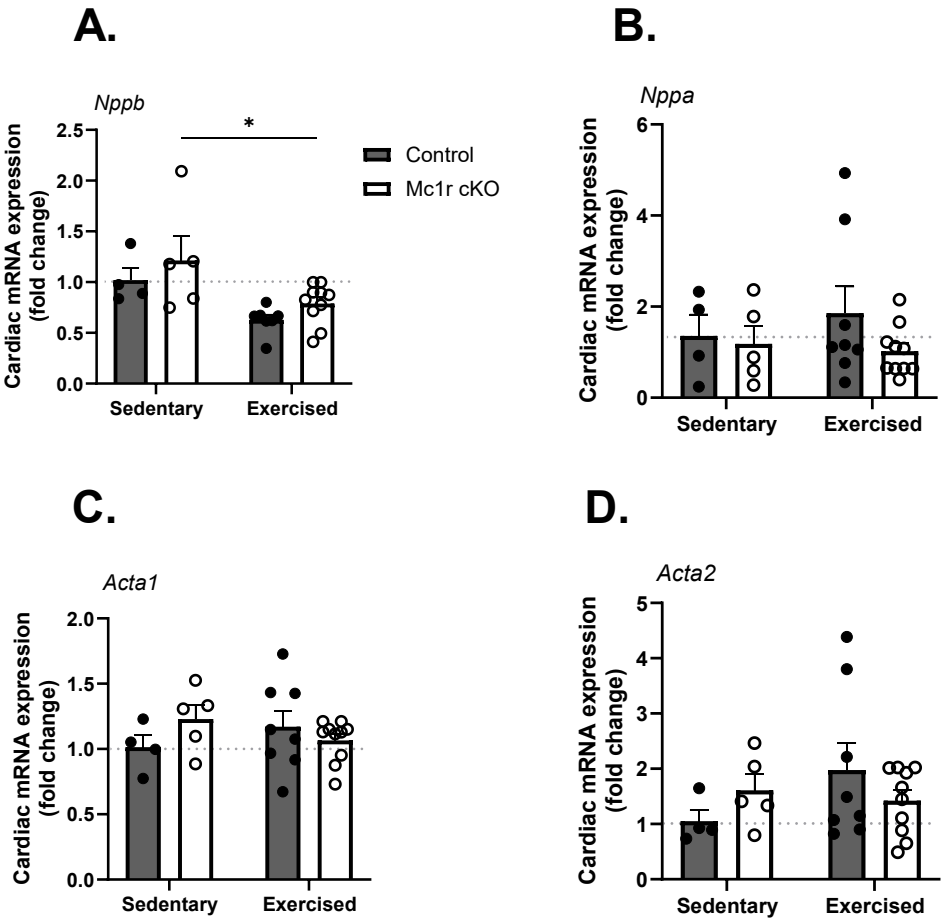

Figure 16. Gene expression profile in Mc1r cKO and control mice. A) *Nppb* (brain natriuretic peptide), B) *Nppa* (atrial natriuretic peptide), C) *Acta1* (skeletal muscle actin), D) *Acta2* (smooth muscle actin) mRNA expression in LV samples. Data are mean ± SEM, each dot represents individual mouse. n=10 in exercised Mc1r cKO mice, n=8 in exercised control mice, n=5 in sedentary Mc1r cKO mice and n=4 in sedentary control mice. Mc1r cKO=cardiomyocyte-specific MC1R knockout. *P<0.05 for the indicated comparisons by 2-way ANOVA and Bonferroni's *post hoc* tests.

Expression of peroxisome proliferator-activated receptor gamma coactivator 1-alpha (*Ppargc1a)* and fibrosis-associated genes, collagen type III alpha 1 chain *(Col3a1),* connective tissue growth factor *(Ctgf),* transforming growth factor *(Tgfb),* and nitric oxide synthase 3 *(Nos3),* were unaffected by either exercise or genotype (figure 17A-E).

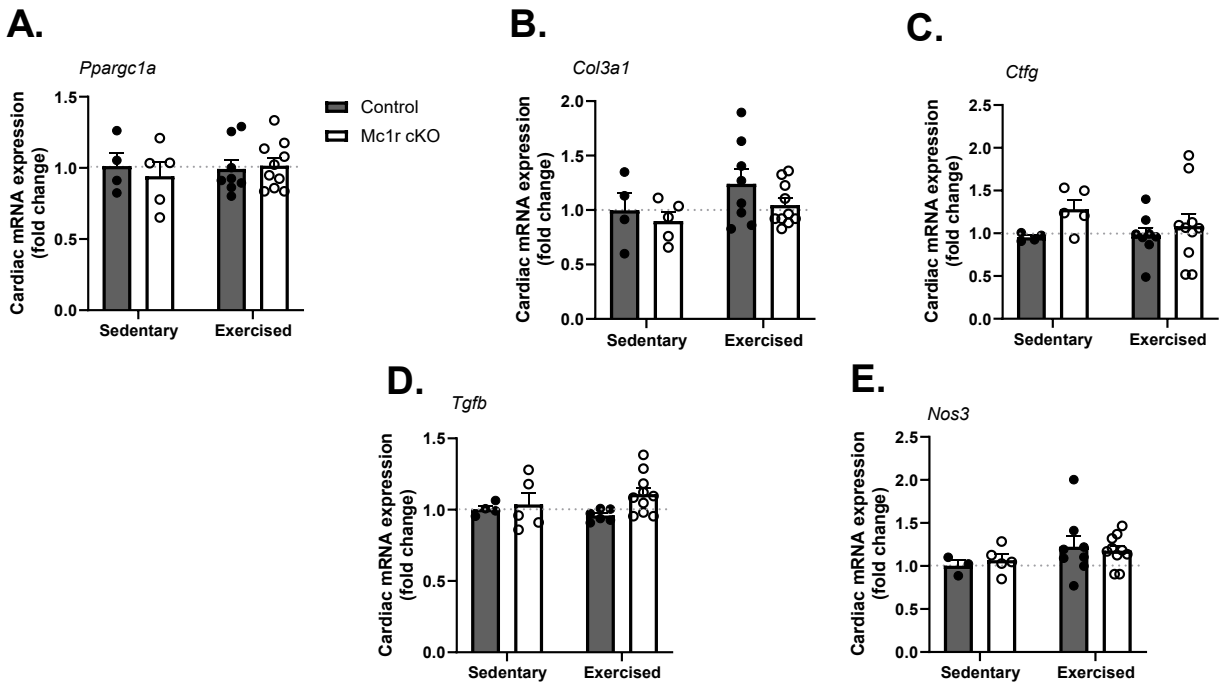

Figure 17. Gene expression profile in Mc1r cKO and control mice. A) *Ppargc1a* (PPARG coactivator 1 alpha), B) *Col3a1* (collagen type III alpha 1 chain), C) *Ctgf* (connective tissue growth factor), D) *Tgfb* (transforming growth factor b), and E) *Nos3* (nitric oxide synthase 3) mRNA expression in LV samples. n=10 in exercised Mc1r cKO mice, n=8 in exercised control mice, n=5 in sedentary Mc1r cKO mice and n=4 in sedentary control mice. Mc1r cKO=cardiomyocyte-specific MC1R knockout. Data are mean ± SEM, each dot represent individual mouse.

Finally, to study changes in fatty acid metabolism, we analysed cardiac mRNA levels of genes related to fatty acid transport into or out of cells, as well as genes related to fatty acid oxidation. Diacyglyserol O-transferase 1 (*Dgat1)* expression was significantly lower in sedentary Mc1r cKO mice compared to control mice, but in exercised group there was no difference between the groups (Figure 18A). Furthermore, the expression of hormone sensitive lipase (*Lipe)* tended (P=0.3311) to increase in exercised Mc1r cKO mice (Figure 18B). Cardiac mRNA levels of other lipid matabolism-related genes are presented in Table 2, but no statistical significances were observed in these genes.

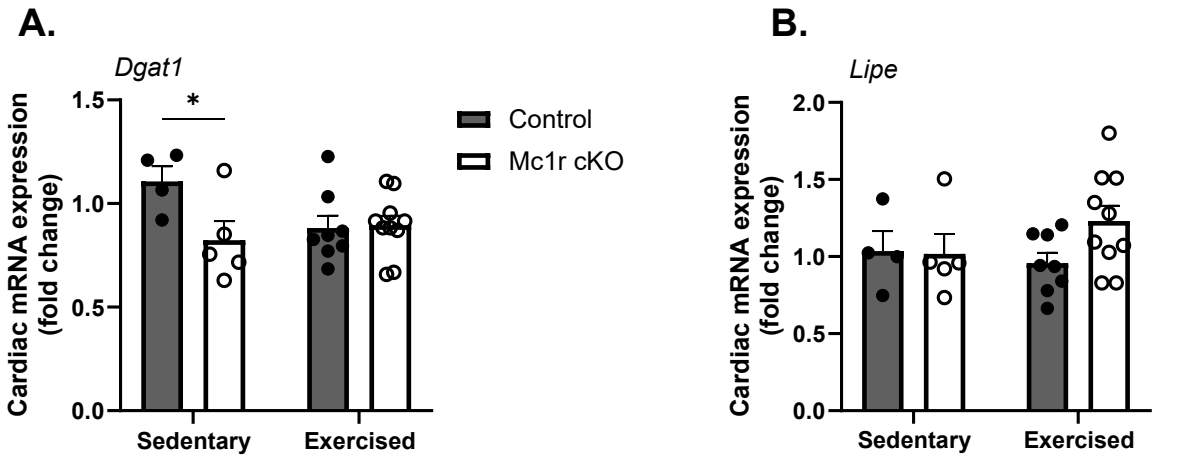

Figure 18. Cardiomyocyte-specific Mc1r knockout decreased *Dgat1* expression in sedentary mice. A) *Dgat1* and B) *Lipe* mRNA expression in LV samples. n=10 in exercised Mc1r cKO mice, n=8 in exercised control mice, n=5 in sedentary Mc1r cKO mice and n=4 in sedentary control mice. Data are mean ± SEM, each dot represent individual mouse. Mc1r cKO=cardiomyocyte-specific MC1R knockout. *P<0.05 for the indicated comparisons by 2-way ANOVA and Bonferroni's *post hoc* tests.

Table 2. Cardiac mRNA expression of lipid metabolism-related genes.

Gene	Sedentary		Exercised	
	Control	Mc1r cKO	Control	Mc1r cKO
Atgl	1.129 ± 0.123	1.152 ± 0.121	1.007 ±0.079	1.188 ±0.082
Cd36	0.998 ±0.066	1.086 ±0.062	1.027 ±0.019	0.979 ±0.033
Cpt1	1.028 ±0.124	1.133 ±0.152	1.099 ±0.101	1.238 ±0.087
Cpt2	1.028 ±0.092	1.135 ±0.032	1.163 ±0.127	1.126 ±0.061
Fas	0.944 ±0.116	0.964 ±0.060	1.184 ±0.077	1.164 ±0.097
Lpl	0.953 ±0.068	1.051 ±0.032	1.015 ±0.022	1.020 ±0.026
Scd1	1.008 ±0.025	1.013 ±0.065	1.042 ±0.111	1.102 ±0.045

Values expressed as mean ±SEM. *Atgl* adipose triglyceride lipase; *Cd36* indicates cluster of differentiation 36; *Cpt1* carnitine palmitoyltransferase 1; *Cpt2* carnitine palmitoyltransferase 2; *Fas* fatty acid synthetase; *Lpl* lipoprotein lipase; *Scd1* stearoyl-CoA desaturase 1. Mc1r cKO=cardiomyocyte-specific MC1R knockout.

3 Discussion

In this study, we examined the role of cardiomyocyte-specific melanocortin 1 receptor in physiological cardiac remodeling utilizing Mc1r cKO mice. The major findings were that EF of Mc1r cKO mice was not improving in response to exercise and LV wall thickness increased less than in control mice. Additionally, Mc1r cKO mice had increased cardiac *Myh7* mRNA and MHC-β protein expressions, which are associated with pathological cardiac remodeling and could potentially explain the lower EF after exercise training.

3.1 The effects of voluntary wheel running and methodological considerations

Here, we used voluntary wheel running to model exercise-induced cardiac responses. Before discussing possible differences in these responses between genotypes, it is important to consider the suitability of this model in the induction of cardiac responses to aerobic exercise. Overall, voluntary wheel running is a well-established method to study exercise-induced skeletal and cardiac responses. However, voluntary nature sets some drawbacks, such as a lack of control over running time, distance, and intensity. Despite these cons, there were no differences in the total running distance between Mc1r cKO and control mice genotypes. Based on this similarity, we can assume, that the exercising stimulus was equal for both genotypes on average. This sets favorable base for further comparison of cardiac responses between genotypes, since similarity of running patterns indicates that any structural or functional changes seen in mice heart are due to genotype effect.

Despite similar running patterns on average, there were major differences in the running volume between individual mice, which may lead to variation in the intensity of exercise-induced cardiac responses. However, high individual differences are not exceptional in this kind of experiments (De Bono et al., 2006), and therefore running results are usually reported as group and average level. Another noteworthy finding related to the model of voluntary wheel running was that our mice, regardless of the genotype, ran remarkably less than what has been reported in the literature (De Bono et al., 2006; Manzanares et al., 2019) (in C57BL/6J mice), or seen in previous voluntary running wheel experiment done in our lab ($Mc1r^{e/e}$ mice run 300km on average). There is possibility for technical reasons which could explain why our mice seemed to run less compared to previous studies. For example, the laptop software might not have counted all the rotations of the running wheels. Differences in running distances could also be

explained by natural mouse strain-specific differences in voluntary running pattern (Goh & Ladiges, 2015). Our mice were on a C57Bl/6J background, and therefore we could assume the running pattern to be quite similar than in C57Bl/6J mice, although cardiomyocyte-specific MC1R knockout may affect it. Nevertheless, 5 weeks is considered to be long enough to induce maximal physiological cardiac hypertrophy, which can be reached with voluntary wheel running (Allen et al., 2001).

Certainly, 5-weeks of voluntary wheel running induced hypertrophic growth of the heart, as evidenced by increase in relative heart weight. This is a more sensitive marker for exercise-trained animals (Allen et al., 2001; Jin et al., 2000) as they are usually leaner than sedentary mice. In literature, 18% increase in heart weight relative to body mass was seen in C57Bl/6J mice after 4 weeks of voluntary wheel running (Allen et al., 2001), which is consistent with our findings in control mice (14% increase).

The effect of exercise was also prominent in terms of intracellular signaling, as we observed increased phosphorylation of AKT in exercised mice compared to sedentary mice. Considering the importance of AKT in hypertrophic signaling, this is a clear sign of exercise-induced changes in the heart. The phosphorylation of AKT is increased by both tyrosine kinase receptor (such as IGF-1 receptors) and GPCR activation as response to exercise (Kemi et al., 2008; McMullen et al., 2003). This phosphorylation is necessary for the induction of exercise-induced physiological cardiac hypertrophy (DeBosch et al., 2006). AKT signaling via mTOR induces cardiomyocyte growth with improved contractile function and enhanced Ca^{2+} handling (Kemi et al., 2008).

Besides AKT, phosphorylation of p38 was increased in exercised mice. Phosphorylation of p38 is known to be induced in cardiomyocytes by several stimuli including endothelin-1, mechanical stress, and other GPCR activation. Furthermore, p38 phosphorylation leads to increased *Nppa* and *Nppb* expression (Kerkelä et al., 2002). However, we did not observe significant increases in these hypertrophic markers due to exercise.

Since our mouse model was created with tamoxifen-inducible Cre-loxP system, it should be taken into account that cardiomyocyte-specific Cre expression itself may have an effect on cardiac structure and function. The induction of cardiomyocyte-specific Cre is associated with adverse effects including systolic dysfunction and cardiac fibrosis (Hall et al., 2011; Lexow et al., 2013). However, these adverse effects seem to be highly dependent on the dose of

tamoxifen. Therefore, our tamoxifen dosing protocol was optimized to induce sufficient gene knockout with minimal adverse effects. Still, despite optimized tamoxifen dosing protocol, some cardiac adverse effects are possible and could falsify our results. Nevertheless, we took this into account by having Cre positive mice with one or zero copies of loxP-targeted *Mc1r* allele as our control group. Consequently, possible Cre-induced cardiac effects are equal in both groups and possible differences in cardiac structure and function are due to cardiac MC1R knockout and not due to cardiac expression of Cre.

3.2 The cardiac phenotype of Mc1r cKO mice

After evaluating the suitability of our mouse model and verifying that the effect of exercising was prominent in mice, we could evaluate the impact of MC1R deficiency on exercise-induced cardiac effects. Absolute ventricular weight was higher in Mc1r cKO mice compared to control mice, but only in sedentary group. Exercise-induced change in absolute ventricular weight was absent in Mc1r cKO (-4% vs. +14% in control mice). Therefore, it seems that genotype affects cardiac hypertrophic response to exercise. Also, LVPW and LVAW thicknesses increased less in Mc1r cKO mice compared to control mice, which further reflects milder increase in heart size. Altogether, based on these observations, it appears that cardiomyocyte-specific MC1R deficiency attenuates the hypertrophic response to exercise training.

Along with attenuated hypertrophic response, ultrasound parameters revealed that cardiomyocyte-specific MC1R deficiency led to deficit in the functional capacity of the heart. We demonstrated that EF was significantly lower in Mc1r cKO mice (+1%) compared to control mice (+ 6,4%) after 5 weeks of voluntary wheel running. Since EF is an essential measure of LV systolic function, calculated by fraction of chamber volume ejected during systole relative to the volume of blood in the ventricle at the end of diastole, it appears that LV systolic function of Mc1r cKO mice is inferior compared to control mice and is uncapable to increase in response to exercise. Attenuated hypertrophic response could explain the lack of improvements in the contractile function of Mc1r cKO mice heart.

In literature, aerobic training, such as running, is associated with eccentric hypertrophy, in which longitudinal cardiomyocyte growth, LV dilatation, and increased cardiac wall thickness are typical (Fernandes et al., 2015; Mihl et al., 2008). In this study, responses to exercise in control mice suggest concentric growth of the heart, as we saw increased LV wall thicknesses and decreased LV diameter. Also, RWT increased after exercise, which is a sign of concentric

hypertrophy (Bernardo et al., 2010). Concentric growth is usually induced by pressure overload caused by resistance or by strength training not by aerobic training (Fernandes et al., 2015; Mihl et al., 2008).

On the contrary, in Mc1r cKO mice we observed slightly increased LV diameter and no change in RWT. Therefore, in Mc1r cKO mice hypertrophic response seemed to be eccentric, or at least concentric hypertrophic response was attenuated. However, we did not measure the length of longitudinal sections of cardiomyocytes, which should increase in LV dilatation and would thus proof the presence of eccentric hypertrophy. Measurement of cardiomyocyte length was not done due to poor quality of H&E sections and the time-limitation to perform additional sections and staining for the analysis. Nevertheless, it is clear that cardiomyocyte-specific MC1R deficiency leads to differences in heart geometry and to compromised LV systolic function.

Possible explanation for reduced systolic LV performance in Mc1r cKO could be related to the expression of myosin heavy chain isoforms in the heart. The expression of *Myh7* gene and MHC-β protein were increased in both sedentary and exercised Mc1r cKO mice compared to control mice. An increase in *Myh7* led to a further decrease in *Myh6/Myh7* ratio in Mc1r cKO mice, which is associated with pathological cardiac hypertrophy both in rodents (Jin et al., 2000) and in human (Lowes et al., 1997; Miyata et al., 2000). Besides this, there is an experimental proof demonstrating that mice overexpressing MHC-β, had mildly reduced cardiac function already under physiological baseline conditions and this difference became more evident after exercise (Krenz & Robbins, 2004). In addition, these mice had mildly dilated LV after exercise, which is in good agreement with the finding in Mc1r cKO mice. Accordingly, increased MHC-β expression could cause LV dilatation and decreased LV performance in Mc1r cKO mice.

Even though we saw differences between Mc1r cKO and control mice, at least in the expression of MHC-β, the underlying intracellular mechanism(s) for the cardiac phenotype of Mc1r cKO mice stays unclear. In terms of intracellular signalling, there were no statistical differences between genotypes in any of studied signaling molecules. However, it seems that JNK phosphorylation tended to increase more in exercised control mice than in Mc1r cKO mice compared to sedentary mice of the same genotype. To be more precise, there was no increase in JNK phosphorylation in exercised Mc1r cKO group compared to sedentary Mc1r cKO group. Therefore, lack of JNK phosphorylation could be explained by MC1R deficiency. However,

further studies are needed to study how MC1R signaling mediates exercise-induced cardiac remodeling.

Lastly, we were interested if presence of cardiac fibrosis could explain lower EF in Mc1r cKO mice compared to control mice besides increased MHC-β expression. Fibrosis is known to lead to stiffness of the myocardium and reduce LV systolic function (Bernardo et al., 2010; González et al., 2018). However, no signs of enhanced fibrosis were observed in the cardiac mRNA levels of fibrosis-related genes or in histological evaluation of H&E-stained sections in Mc1r cKO mice. Although we did not observe fibrosis, most probably there are still other undiscovered differences between the genotypes, which could further explain lower systolic function in Mc1r cKO mice.

3.3 Translational insights and therapeutic perspectives

Our findings might have translational relevance as *MC1R* is highly polymorphic gene in humans and several dysfunctional *MC1R* variants have been identified. Previous studies have shown that dysfunctional MC1R leads to similar effects in mice and human. In addition to similar changes in melanin synthesis (Dessinioti et al., 2011; Wolf Horrell et al., 2016), deficiency of MC1R leads to vascular dysfunction in both mice and human (Rinne et al., 2015). Therefore, it is possible that humans carrying dysfunctional MC1R could express, at least to some extent, similar phenotype as observed in this study in mice.

Exercise is known to be an excellent way to maintain healthy lifestyle as well as the most effective nonpharmacological intervention to reduce CVD (Nystoriak & Bhatnagar, 2018; Rivera-Brown & Frontera, 2012; Seo et al., 2020). Considering that MC1R appears to have a role in mediating exercise-induced hypertrophic responses and systolic function of the heart, MC1R could, in theory, be pharmacologically targeted to maintain or enhance cardiac responses to exercise. Not surprisingly, there has been an interest in developing exercise mimetics, drugs aiming to induce exercise-like effects, as a treatment strategy for CVDs, such as for pathological cardiac hypertrophy and heart failure (Gubert & Hannan, 2021). MC1R could be one possible target for exercise mimetic drugs for treatment of these diseases.

Although MC1R-mediated induction of physiological cardiac remodeling is ambitious treatment strategy to improve cardiac function of heart failure patients, it is clear that heart failure patients would benefit from exercise mimetics. Heart failure patients are often unable to exercise due to severe exercise intolerance and other comorbidities. In addition, compliance

with exercise programs is often poor, supporting the need for exercise mimetics. In patients with mild heart failure, exercise mimetics could be combined with lifestyle intervention leading to the best treatment response.

Currently, drug treatments for heart failure and pathological hypertrophy are mostly delaying the progression of the disease rather than curing it and mortality due to heart failure stays high (McMurray & Pfeffer, 2005). This highlights the need for drugs which enhance cardiac function and improve the survival of heart failure patients. However, further research is needed to establish mechanistical roles of MC1R in both physiological and pathological hypertrophy to be able to develop safe and effective MC1R targeted drugs.

Use of melanocortin drugs is not limited to cardiovascular diseases, since melanocortins have several roles in human physiology. α-MSH analogues are already approved for clinical use in skin disorders, sexual disorders and obesity (Montero-Melendez et al., 2022). These α-MSH analogues have agonistic activity also for MC1R and therefore, it is important to evaluate the potential cardiac effects of these drugs. Similarly, cardiac effects of future melanocortin drugs for other than cardiovascular indications should be evaluated to minimize possible adverse effects.

3.4 Conclusions

In conclusion, this study suggests that cardiomyocyte-specific MC1R deficiency attenuates hypertrophic response to exercise training and reduces heart's capacity to improve systolic function. Mechanistic explanation for these results stays unclear, although increased MHC-β expression may be one causative factor. These results may have translational significance as *MC1R* has several dysfunctional variants in humans, which could be associated with an impairment in exercise-induced cardiac effects.

4 Materials and methods

4.1 Mouse model

In this study, we used an inducible cardiomyocyte-specific MC1R knockout mouse model (Mc1r cKO). The model was created by crossbreeding Mc1r floxed mice ($Mc1r^{fl/fl}$, Jacksons Laboratory) with tamoxifen-inducible Myh6-MerCreMer transgenic mice (Myh6-MCM, Jacksons Laboratory). Myh6-MCM mice express a tamoxifen-inducible Cre recombinase protein, which is fused to two mutant human estrogen-receptor ligand-binding domains (MerCreMer). Estrogen-receptor ligand-binding domains are expressed under the control of myosin heavy chain 6 (*Myh6*) promoter. $Mc1r^{fl/fl}$ mice, on the other hand, have melanocortin 1 receptor genes flanked with recombinase recognition sequences (loxP sites for Cre). Crossing of these mice produced several possible genotypes but gene knockout can take place only in Myh6 $^{+/-}$ $Mc1r^{fl/fl}$ mice. (Sohal et al., 2001.) Gene knockout was induced in 8-week-old male mice through intraperitoneal administration of tamoxifen (Cayman Chemicals, Ann Arbor, MI, # 13258) for four consecutive days (20 mg/kg/day dissolved in peanut oil). Dosing was followed by a one-week recovery period.

The study involved two experimental arms: exercise group that had access to a running wheel for 5 weeks and a sedentary group that had the same but non-rotating running wheels. The running group included 11 Mc1r cKO mice ($Myh6^{+/-}Mc1r^{fl/fl}$ mice) and 8 control mice ($Myh6^{+/-}$ $Mc1r^{-/-}$). The sedentary group included 5 Mc1r cKO mice and 5 control mice ($MYH6^{+/-}$ $Mc1r^{-/-}$ or $MYH6^{-/-}$ $Mc1r^{-/-}$).

Mice were individually housed (due to running wheel installation) and maintained on a 12 h light/dark cycle, with access to food (2916C Teklad Global diet, Envigo) and tap water ad libitum. All experiments were approved by the national Animal Experiment Board in Finland (License number: ESAVI/45421/2022) and conducted in compliance with the Directive 2010/63/EU of the European Parliament regarding the protection of animals used for scientific purposes, and with the institutional and national guidelines for the care and use of laboratory animals.

4.2 Running wheel experiment

To induce physiological cardiac hypertrophy, mice were subjected to voluntary wheel running for duration of 5 weeks (35 days). Angled running wheels (Low Profile Wireless Running

Wheel for Mice, ENV-004, Med Associates Inc., Figure 19) were installed in the individually ventilated cages after baseline echocardiography. Running wheels had a sensor that calculated the rounds and sent the data (=counts and time) to a hub (Wireless Running wheel USB Interface HUB, DIG-804, Med Associates Inc.) attached to a computer program (Wheel manager software, SOF-860, Med Associates Inc.). Data from average running time and distance in day and cumulative running distance during the experiment were analyzed. Mice in the sedentary group had running wheels with stoppers.

Figure 19. Demonstrative image of angled running wheel setup. Image from Med associates Inc. (https://med-associates.com/product/low-profile-wireless-running-wheel/)

4.3 Echocardiography

Cardiac structure and function were evaluated by transthoracic echocardiography (Vevo 2100, Visual Sonics Inc., Toronto, Canada) in mice before running intervention and five weeks after running. Imaging was performed under isoflurane anesthesia (induction 4%, maintenance 1-1,5%) (Attane vet 1000mg/g, Piramal healthcare UK Limited, UK). PSLAX and SAX B-mode and M-mode images as well as pulsed wave and tissue doppler images were taken and analysed using VevoLab (version 5.5.0) software in a blinded manner. Relative wall thickness (RWT) was calculated as (LV posterior wall thickness + LV anterior wall thickness)/LV end-diastolic dimension. Further sorting of the data was performed using Excel and statistical analysis with Graph Pad Prism version 8.0 (La Jolla, Ca, USA).

4.4 Histology

Immediately after sacrificing mice with CO_2, the hearts were excised, weighed, and transversely cut. The base of the heart was put into 10% formalin for fixation overnight, after which it was moved to 70% EtOH for dehydration. This was followed by paraffin embedding and sectioning to four µm-thick sections. Sections were stained with hematoxylin and eosin (H&E). Histological methods were performed by the Histology core facility of the Institute of Biomedicine, University of Turku, Finland.

Stained sections were scanned with Pannoramic P1000 digital slide scanner (3DHISTECH Kft, Budapest, Hungary). Aquired images were used to quantify cross sectional area of cardiomyocytes using Case Viewer software (3DHISTECH Kft, Budapest, Hungary). Transverse-cut cardiomyocytes (at least 100 cells per mouse) with nuclei in the middle or near the middle were selected for the analysis.

4.5 RNA isolation, cDNA synthesis, and quantitative RT-PCR

After sacrificing mice as described above, the heart apex was fast-frozen in liquid nitrogen and stored at −70°C for subsequent RNA extraction. Initially, apex samples were homogenized with Qiazol Lysis reagent (Qiagen) using the Qiagen TissueLyser LT Bead Mill (QIAGE, Venlo, Netherlands), after which total RNA was extracted from each sample utilizing Direct-zol RNA Miniprep (Zymo Research, CA, USA). Finally, the quality and concentration of RNA were evaluated by Nanodrop.

The RNA was reverse-transcribed to cDNA with a Primescripts RT kit (Takara Clontech) according to the manufacturer's instructions. Quantitative real-time polymerase chain reaction (RT-qPCR) with SYBR green protocols (Kapa Biosystems, MA, USA) was used to perform gene expression analysis with real-time PCR detection system (Applied Biosystems 7300 Real-Time PCR system).

The expression of target genes expression was normalized to the geometric mean of two housekeeping genes (b-actin and 18S) using delta-Ct method. Results are decipted as relative transcript levels ($2^{-\Delta\Delta Ct}$).
Primer sequences are presented in Tables 3 and 4.

Table 3. Quantitative RT-PCR primers for mouse genes.

Gene name	Accession number	Full name	Forward	Reverse
Acta1	NM_001272041.1	Actin, alpha skeletal muscle	cccaaagctaaccgggagaag	ccagaatccaacacgatgcc
Acta2	NM_007392.3	Actin, alpha 2, smooth muscle, aorta	agattgtgcgcgacatcaaag	gcagactccataccgataaagga
Atgl	NM_001163689.1	Adipose triglyseride lipase	caacgccactcacatctacgg	ggacacctcaataatgttggcac
Atp2a2	NM_001110140.3	Calcium-ATPase type 2 in sarco-/endoplasmic reticulum	gagaacgctcacacaaagacc	cttcttcagccggcaattcgttg
Cd36	NM_001159558.1	Cluster determinant 36 / fatty acid translocase (FAT)	ccaagctattgcgacatgatt	tctcaatgtccgagacttttca
Col3a1	NM_009930.2	Collagen type III alpha chain 1	ctaaaattctgccaccccgaa	aggatcaacccagtattctccactc
Cpt1	NM_013495.2	Carnitine palmitoyltransferase 1	gctgtcaaagataccgtgagc	tctccctccttcatcagtgg
Cpt2	NM_009949.2	Carnitine palmitoyltransferase 2	cagcacagcatcgtacca	cccaatgccgttctcaaaa
Ctgf	NM_010217.2	Connective tissue growth factor	agacctgtgggatgggcat	gcttggcgattttaggtgtcc
Dgat1	NM_010046.4	Diacylglycerol O-acyltransferase	gccacaatcatctgcttccc	ccactgaccttcttcctgt
Fas	NM_007988.3	Fatty acid synthase	gctgctgttggaagtcagc	agtgttcgttcctcggagtg
Lipe	NM_001039507.2	Hormone-sensitive lipase	gcgctggaggagtgttttt	cgctctccagttgaaccaag
Lpl	NM_008509.2	Lipoprotein lipase	ctcgctctcagatgccctac	aggcctggttgtgttgctt
Mc1r	NM_008559.2	Melanocortin receptor 1	gtgctggttgtgatagccatc	tgctgacacttaccatcaggt
Myh6	NM_010856.4	Myosin heavy chain polypeptide 6	ccacttctccttggtccactatg	acaaacccaccaccgtctca
Myh7	NM_080728.3	Myosin heavy chain polypeptide 7	agggtggcaaagtcactgct	catcacctggtcctccttca
Nos3	NM_008713.4	Nitric oxide synthase 3	ggcactgctgagccgagtgg	gagcctgccgcagcgtacat
Nppa	NM_008725.3	Atrial natriuretic peptide	gcttccaggccatattggag	gggggcatgacctcatctt
Nppb	NM_008726.6	Brain natriuretic peptide	cccaaaaagagtccttcggtc	cggtctatcttgtgcccaaag
Ppargc1a	NM_008904.3	PPARG coactivator 1 Alpha	tatggagtgacatagagtgtgct	ccacttcaatccacccagaaag
Scd1	NM_009127.4	Stearoyl-CoA desaturase	cattctcatggtcctgctgc	tgccttgtaagttctgtggc

Tgfb1	NM_011577.2	Transforming growth factor beta 1	ccgcaacaacgccatctatg	cccgaatgtctgacgtattgaag

Table 4. Quantitative RT-PCR primers for mouse housekeeping genes.

Gene name	Accession number	Full name	Forward	Reverse
ACTB	NM_007393.5	Actin beta	tccatcatgaagtgtgacgt	gagcaatgatcttgatcttca
S29	NM_009093.2	40S ribosomal protein S29	atgggtcaccagcagctcta	agcctatgtccttcgcgtact

4.6 Western blotting

After sacrificing mice as described above, the apex of the heart was fast-frozen in liquid nitrogen and stored at −70°C for total protein extraction. Heart apex samples were homogenized in RIPA buffer complemented with phosphatase and protease inhibitor cocktail (Complete Mini, Roche and Halt™ Phosphatase Inhibitor Cocktail, ThermoFisher) utilizing the Qiagen TissueLyser LT Bead. Protein concentrations in the samples were determined with BSA protein assay (Thermo Scientific, USA) according to the manufacturer's instructions.

Equal amounts of total protein (30 µg) were separated by 10% or 15% SDS-polyacrylamide gel electrophoresis (SDS-PAGE) after which transferred onto PVDF membranes (Immun-Blot PVDF Membrane, Biorad). After blocking with Tris-Buffered Saline containing 0.1% Tween 20 detergent (Sigma-Aldrich) and 5% skimmed milk (Valio) or 3% bovine serum albumin (Tocris, UK) for 1 hr at room temperature (RT), membranes were incubated with specific primary antibodies (Table 5) for overnight at +4 °C.

Table 5. Primary antibodies used in the experiment.

Target	Cat No	Source	Dilution	Company
p-AKT	AF887-SP	Rabbit	1:500	R&D systems
total-AKT	MAB2055-SP	Rabbit	1:500	R&D systems
p-AMPK	2535	Rabbit	1:600	Cell signaling
total-AMPK	2532	Rabbit	1:1000	Cell signaling
BNP	ABIN7010021	Rabbit	1:2000	Antibodies-online
p-CREB	MA5-11192	Rabbit	1:1000	ThermoFisher
total-CREB	9197	Rabbit	1:1000	Cell signaling
p-ERK	9107	Mouse	1:1000	Cell signaling
total-ERK	9106	Mouse	1:1000	Cell signaling
GAPDH	ab181602	Rabbit	1:5000	Abcam

p-JNK	MAB1205-SP	Rabbit	1:750	R&D systems
total-JNK	AF-1387-SP	Rabbit	1:1500	R&D systems
MHCa	ab50976	Mouse	1:1000	Abcam
MHCb	ab11083	Mouse	1:600	Abcam
PGC1a	NBP1-04676	Rabbit	1:100	Novusbio
p-p38	9215	Rabbit	1:750	Cell signaling
total-p38	9212	Rabbit	1:750	Cell signaling
β-actin	A2066	Rabbit	1:2000	Merk Life Science Oy

Following day, membranes were washed and incubated with horseradish peroxidase (HRP)-conjugated secondary antibodies (Table 6) in dilution 1:2000 for 1 hr at RT. Next, proteins were detected with a chemiluminescence ECL substrate (Bio Rad). Target protein concentration was normalized to correct for loading either to GAPDH or β-actin. ImageJ software (NIH, Bethesda, MD, USA) was used to analyse band densities. Membranes were stripped using Abcam's stripping protocol and mild stripping buffer.

Table 6. Secondary antibodies used in the experiment.

Target	Cat No	Dilution	Company
Anti-rabbit IgG HRP-linked	7074	1:2000	Cell signalling
Anti-mouse IgG HRP-linked	7076	1:2000	Cell signalling

4.7 Statistical analysis

Statistical analyses were performed with GraphPad Prism 8 software (La Jolla, Ca, USA). The statistical significance between groups was defined using unpaired Student's t-test or two-way ANOVA followed by Bonferroni's *post hoc* tests. Possible outliers in the data sets were recognized using the regression and outlier removal (ROUT) method of Q-level of 1%. Data are expressed as mean ± standard error of the mean (SEM). Results are considered statistically significant for $P<0.05$.

5 Acknowledgements

This research has been made possible with the supervision and mentoring from Petteri Rinne and Anni Suominen.
Thanks also to Keshav Thapa and Sanna Bastman for experimental and technical support.

6 Abbreviations list

Acta1 – skeletal alpha actin (gene)

Acta2 – smooth muscle actin (gene)

ACTH - adrenocorticotropic hormone

Akt – alpha serine/threonine-protein kinase

AMPK – AMP-activated protein kinase

Ang II – angiotensin II

ANP – atrial natriuretic peptide

B-mode – brightness mode

BNP – brain natriuretic peptide

cAMP – cyclic adenosine monophosphate

CNS – central nervous system

CO – cardiac output

Col3a1 – collagen type III alpha 1 chain (gene)

Ctgf – connective tissue growth factor

CVD – cardiovascular disease

Dgat1 – diacyglyserol O-transferase 1

EF – ejection fraction

eNOS – endothelial nitric oxide synthase

ERK1/2- extracellular signal-regulated kinases 1/2

FS – fractional shortening

GAPDH – glyceraldehyde-3-phosphate-dehydrogenase

GPCR – G-protein coupled receptor

H&E – hematoxylin and eosin

IGF1 – insulin-like growth factor 1

Lipe – hormone sensitive lipase

Lpl – lipoprotein lipase

LVAW – left ventricular anterior wall thickness

LVEDD – left ventricular end-diastolic diameter

LVESD – left ventricular end-systolic diameter

LVPW – left ventricular posterior wall thickness

LV – left ventricle

MAPK – mitogen-activated protein kinase

Mc1r cKO – cardiomyocyte-specific melanocortin 1 receptor knockout

Mc1r $^{e/e}$ – recessive MC1R mouse

MC1R-MC5R – melanocortin 1-5 receptor (protein)

Mc1r – melanocortin 1 receptor (mouse gene)

MHCα – myosin heavy chain alpha

MHCβ – myosin heavy chain beta

M-mode – motion mode

MV A – late diastolic flow velocity, active filling

MV E/A – transmitral flow velocity ratio of early (passive) filling and late (active) filling

MV E – early diastolic flow velocity, passive filling

Myh7 – myosin heavy chain 7 (gene)

Nos3 – nitric oxide synthase 3

Nppa – atrial natriuretic peptide (gene)

Nppb – brain natriuretic peptide (gene)

p-AKT – phosphorylated AKT

p-AMKP – phosphorylated AMPK

p-CREB – phosphorylated cAMP-response element binding protein

p-ERK – phosphorylated ERK

PGC1a – peroxisome proliferator-activated receptor y co-activator 1a

PI3K – phosphoinositide-3-kinase

PKA – protein kinase A

PLAX – parasternal long-axis

POMC – proopiomelanocortin

Ppargc1a – peroxisome proliferator-activated receptor gamma coactivator 1-aplha (gene)

p-p38 – phosphorylated p38

PSAX – parasternal short-axis

qRT-PCR – quantitative real time polymerase chain reaction

RWT – relative wall thickness

SV – stroke volume

TAC - transverse aortic constriction

Tgfb – transforming growth factor

α-MSH – α-melanocyte stimulating hormone

β-MSH – β-melanocyte stimulating hormone

γ-MSH - γ-melanocyte stimulating hormone

References

Allen, D. L., Harrison, B. C., Maass, A., Bell, M. L., Byrnes, W. C., & Leinwand, L. A. (2001). Cardiac and skeletal muscle adaptations to voluntary wheel running in the mouse. *Journal of Applied Physiology*, *90*(5), 1900–1908. https://doi.org/10.1152/jappl.2001.90.5.1900

Baggish, A. L., Wang, F., Weiner, R. B., Elinoff, J. M., Tournoux, F., Boland, A., Picard, M. H., Hutter, A. M., & Wood, M. J. (2008). Training-specific changes in cardiac structure and function: A prospective and longitudinal assessment of competitive athletes. *Journal of Applied Physiology*, *104*(4), 1121–1128. https://doi.org/10.1152/japplphysiol.01170.2007

Basso, C., Michaud, K., d'Amati, G., Banner, J., Lucena, J., Cunningham, K., Leone, O., Vink, A., Van Der Wal, A. C., Sheppard, M. N., & on behalf of the Association for European Cardiovascular Pathology. (2021). Cardiac hypertrophy at autopsy. *Virchows Archiv*, *479*(1), 79–94. https://doi.org/10.1007/s00428-021-03038-0

Bernal-Ramirez, J., Díaz-Vesga, M. C., Talamilla, M., Méndez, A., Quiroga, C., Garza-Cervantes, J. A., Lázaro-Alfaro, A., Jerjes-Sanchez, C., Henríquez, M., García-Rivas, G., & Pedrozo, Z. (2021). Exploring Functional Differences between the Right and Left Ventricles to Better Understand Right Ventricular Dysfunction. *Oxidative Medicine and Cellular Longevity*, *2021*, 1–21. https://doi.org/10.1155/2021/9993060

Bernardo, B. C., Weeks, K. L., Pretorius, L., & McMullen, J. R. (2010). Molecular distinction between physiological and pathological cardiac hypertrophy: Experimental findings and therapeutic strategies. *Pharmacology & Therapeutics*, *128*(1), 191–227. https://doi.org/10.1016/j.pharmthera.2010.04.005

Buscà, R., & Ballotti, R. (2000). Cyclic AMP a Key Messenger in the Regulation of Skin Pigmentation: Cyclic AMP and Skin Pigmentation. *Pigment Cell Research*, *13*(2), 60–69. https://doi.org/10.1034/j.1600-0749.2000.130203.x

Catania, A., Gatti, S., Colombo, G., & Lipton, J. M. (2004). Targeting Melanocortin Receptors as a Novel Strategy to Control Inflammation. *Pharmacological Reviews*, *56*(1), 1–29. https://doi.org/10.1124/pr.56.1.1

Chai, B., Li, J.-Y., Zhang, W., Ammori, J. B., & Mulholland, M. W. (2007). Melanocortin-3 receptor activates MAP kinase via PI3 kinase. *Regulatory Peptides*, *139*(1–3), 115–121. https://doi.org/10.1016/j.regpep.2006.11.003

Chen, H., Chen, C., Spanos, M., Li, G., Lu, R., Bei, Y., & Xiao, J. (2022). Exercise training maintains cardiovascular health: Signaling pathways involved and potential therapeutics. *Signal Transduction and Targeted Therapy*, *7*(1), 306. https://doi.org/10.1038/s41392-022-01153-1

Chhajlani. (1996). Distribution of cDNA for melanocortin receptor subtypes in human tissues. *Biochemistry and Molecular Biology International*, *38(1):73-80*.

Cooray, S. N., & Clark, A. J. L. (2011). Melanocortin receptors and their accessory proteins. *Molecular and Cellular Endocrinology*, *331*(2), 215–221. https://doi.org/10.1016/j.mce.2010.07.015

De Bono, J. P., Adlam, D., Paterson, D. J., & Channon, K. M. (2006). Novel quantitative phenotypes of exercise training in mouse models. *American Journal of Physiology-Regulatory, Integrative and Comparative Physiology*, *290*(4), R926–R934. https://doi.org/10.1152/ajpregu.00694.2005

DeBosch, B., Treskov, I., Lupu, T. S., Weinheimer, C., Kovacs, A., Courtois, M., & Muslin, A. J. (2006). Akt1 Is Required for Physiological Cardiac Growth. *Circulation*, *113*(17), 2097–2104. https://doi.org/10.1161/CIRCULATIONAHA.105.595231

Dessinioti, C., Antoniou, C., Katsambas, A., & Stratigos, A. J. (2011). Melanocortin 1 Receptor Variants: Functional Role and Pigmentary Associations: Photochemistry and Photobiology. *Photochemistry and Photobiology*, *87*(5), 978–987. https://doi.org/10.1111/j.1751-1097.2011.00970.x

Epstein, F. H., Levin, E. R., Gardner, D. G., & Samson, W. K. (1998). Natriuretic Peptides. *New England Journal of Medicine*, *339*(5), 321–328. https://doi.org/10.1056/NEJM199807303390507

Fernandes, T., Baraúna, V. G., Negrão, C. E., Phillips, M. I., & Oliveira, E. M. (2015). Aerobic exercise training promotes physiological cardiac remodeling involving a set of microRNAs. *American Journal of Physiology-Heart and Circulatory Physiology*, *309*(4), H543–H552. https://doi.org/10.1152/ajpheart.00899.2014

Goh, J., & Ladiges, W. (2015). Voluntary Wheel Running in Mice. *Current Protocols in Mouse Biology*, *5*(4), 283–290. https://doi.org/10.1002/9780470942390.mo140295

González, A., Schelbert, E. B., Díez, J., & Butler, J. (2018). Myocardial Interstitial Fibrosis in Heart Failure. *Journal of the American College of Cardiology*, *71*(15), 1696–1706. https://doi.org/10.1016/j.jacc.2018.02.021

Grant, M. D., Mann, R. D., Kristenson, S. D., Buck, R. M., Mendoza, J. D., Reese, J. M., Grant, D. W., & Roberge, E. A. (2021). Transthoracic Echocardiography: Beginner's Guide with Emphasis on Blind Spots as Identified with CT and MRI. *RadioGraphics*, *41*(4), E1022–E1042. https://doi.org/10.1148/rg.2021200142

Gubert, C., & Hannan, A. J. (2021). Exercise mimetics: Harnessing the therapeutic effects of physical activity. *Nature Reviews Drug Discovery*, *20*(11), 862–879. https://doi.org/10.1038/s41573-021-00217-1

Hall, M. E., Smith, G., Hall, J. E., & Stec, D. E. (2011). Systolic dysfunction in cardiac-specific ligand-inducible MerCreMer transgenic mice. *American Journal of Physiology-Heart and Circulatory Physiology*, *301*(1), H253–H260. https://doi.org/10.1152/ajpheart.00786.2010

Hillis, G. S., & Bloomfield, P. (2005). Basic transthoracic echocardiography. *BMJ*, *330*(7505), 1432–1436. https://doi.org/10.1136/bmj.330.7505.1432

Jin, H., Yang, R., Li, W., Lu, H., Ryan, A. M., Ogasawara, A. K., Van Peborgh, J., & Paoni, N. F. (2000). Effects of exercise training on cardiac function, gene expression, and apoptosis in rats. *American Journal of Physiology-Heart and Circulatory Physiology*, *279*(6), H2994–H3002. https://doi.org/10.1152/ajpheart.2000.279.6.H2994

Kemi, O. J., Ceci, M., Wisloff, U., Grimaldi, S., Gallo, P., Smith, G. L., Condorelli, G., & Ellingsen, O. (2008). Activation or inactivation of cardiac Akt/mTOR signaling diverges physiological from pathological hypertrophy. *Journal of Cellular Physiology*, *214*(2), 316–321. https://doi.org/10.1002/jcp.21197

Kemi, O. J., Loennechen, J. P., Wisløff, U., & Ellingsen, Ø. (2002). Intensity-controlled treadmill running in mice: Cardiac and skeletal muscle hypertrophy. *Journal of Applied Physiology*, *93*(4), 1301–1309. https://doi.org/10.1152/japplphysiol.00231.2002

Kerkelä, R., Pikkarainen, S., Majalahti-Palviainen, T., Tokola, H., & Ruskoaho, H. (2002). Distinct Roles of Mitogen-activated Protein Kinase Pathways in GATA-4 Transcription Factor-mediated Regulation of B-type Natriuretic Peptide Gene. *Journal of Biological Chemistry*, *277*(16), 13752–13760. https://doi.org/10.1074/jbc.M105736200

Kim, J. H., Kiefer, L. L., Woychik, R. P., Wilkison, W. O., Truesdale, A., Ittoop, O., Willard, D., Nichols, J., & Zemel, M. B. (1997). Agouti regulation of intracellular calcium: Role of melanocortin receptors. *American Journal of Physiology-Endocrinology and Metabolism*, *272*(3), E379–E384. https://doi.org/10.1152/ajpendo.1997.272.3.E379

Krenz, M., & Robbins, J. (2004). Impact of beta-myosin heavy chain expression on cardiac function during stress. *Journal of the American College of Cardiology*, *44*(12), 2390–2397. https://doi.org/10.1016/j.jacc.2004.09.044

Lee, A. A., Dillmann, W. H., McCulloch, A. D., & Villarreal, F. J. (1995). Angiotensin II stimulates the autocrine production of transforming growth factor-β1 in adult rat cardiac fibroblasts. *Journal of Molecular and Cellular Cardiology*, *27*(10), 2347–2357. https://doi.org/10.1016/S0022-2828(95)91983-X

Lexow, J., Poggioli, T., Sarathchandra, P., Santini, M. P., & Rosenthal, N. (2013). Cardiac fibrosis in mice expressing an inducible myocardial-specific Cre driver. *Disease Models & Mechanisms*, dmm.010470. https://doi.org/10.1242/dmm.010470

Lindsey, M. L., Kassiri, Z., Virag, J. A. I., De Castro Brás, L. E., & Scherrer-Crosbie, M. (2018). Guidelines for measuring cardiac physiology in mice. *American Journal of Physiology-Heart and Circulatory Physiology*, *314*(4), H733–H752. https://doi.org/10.1152/ajpheart.00339.2017

Lowes, B. D., Minobe, W., Abraham, W. T., Rizeq, M. N., Bohlmeyer, T. J., Quaife, R. A., Roden, R. L., Dutcher, D. L., Robertson, A. D., Voelkel, N. F., Badesch, D. B., Groves, B. M., Gilbert, E. M., & Bristow, M. R. (1997). Changes in gene expression in the intact human heart. Downregulation of alpha-myosin heavy chain in hypertrophied, failing ventricular myocardium. *Journal of Clinical Investigation*, *100*(9), 2315–2324. https://doi.org/10.1172/JCI119770

Lyons, G. E., Schiaffino, S., Sassoon, D., Barton, P., & Buckingham, M. (1990). Developmental regulation of myosin gene expression in mouse cardiac muscle. *The Journal of Cell Biology*, *111*(6), 2427–2436. https://doi.org/10.1083/jcb.111.6.2427

Maillet, M., Van Berlo, J. H., & Molkentin, J. D. (2013). Molecular basis of physiological heart growth: Fundamental concepts and new players. *Nature Reviews Molecular Cell Biology*, *14*(1), 38–48. https://doi.org/10.1038/nrm3495

Manzanares, G., Brito-da-Silva, G., & Gandra, P. G. (2019). Voluntary wheel running: Patterns and physiological effects in mice. *Brazilian Journal of Medical and Biological Research*, *52*(1), e7830. https://doi.org/10.1590/1414-431x20187830

Massett, M. P., Matejka, C., & Kim, H. (2021). Systematic Review and Meta-Analysis of Endurance Exercise Training Protocols for Mice. *Frontiers in Physiology*, *12*, 782695. https://doi.org/10.3389/fphys.2021.782695

McMullen, J. R., Shioi, T., Zhang, L., Tarnavski, O., Sherwood, M. C., Kang, P. M., & Izumo, S. (2003). Phosphoinositide 3-kinase(p110α) plays a critical role for the induction of physiological, but not pathological, cardiac hypertrophy. *Proceedings of the National Academy of Sciences*, *100*(21), 12355–12360. https://doi.org/10.1073/pnas.1934654100

McMurray, J. J., & Pfeffer, M. A. (2005). Heart failure. *The Lancet*, *365*(9474), 1877–1889. https://doi.org/10.1016/S0140-6736(05)66621-4

Mihl, C., Dassen, W. R. M., & Kuipers, H. (2008). Cardiac remodelling: Concentric versus eccentric hypertrophy in strength and endurance athletes. *Netherlands Heart Journal*, *16*(4), 129–133. https://doi.org/10.1007/BF03086131

Miyata, S., Minobe, W., Bristow, M. R., & Leinwand, L. A. (2000). Myosin Heavy Chain Isoform Expression in the Failing and Nonfailing Human Heart. *Circulation Research*, *86*(4), 386–390. https://doi.org/10.1161/01.RES.86.4.386

Montero-Melendez, T., Boesen, T., & Jonassen, T. E. N. (2022). Translational advances of melanocortin drugs: Integrating biology, chemistry and genetics. *Seminars in Immunology*, *59*, 101603. https://doi.org/10.1016/j.smim.2022.101603

Moran, C. M., Thomson, A. J. W., Rog-Zielinska, E., & Gray, G. A. (2013). High-resolution echocardiography in the assessment of cardiac physiology and disease in preclinical models. *Experimental Physiology*, *98*(3), 629–644. https://doi.org/10.1113/expphysiol.2012.068577

Morganroth, J. (1975). Comparative Left Ventricular Dimensions in Trained Athletes. *Annals of Internal Medicine*, *82*(4), 521. https://doi.org/10.7326/0003-4819-82-4-521

Mountjoy, K. G., Robbins, L. S., Mortrud, M. T., & Cone, R. D. (1992). The Cloning of a Family of Genes That Encode the Melanocortin Receptors. *Science*, *257*(5074), 1248–1251. https://doi.org/10.1126/science.1325670

Nemoto, S., Sheng, Z., & Lin, A. (1998). Opposing Effects of Jun Kinase and p38 Mitogen-Activated Protein Kinases on Cardiomyocyte Hypertrophy. *Molecular and Cellular Biology*, *18*(6), 3518–3526. https://doi.org/10.1128/MCB.18.6.3518

Neri Serneri, G. G., Boddi, M., Modesti, P. A., Cecioni, I., Coppo, M., Padeletti, L., Michelucci, A., Colella, A., & Galanti, G. (2001). Increased Cardiac Sympathetic Activity and Insulin-Like Growth Factor-I Formation Are Associated With Physiological Hypertrophy in Athletes. *Circulation Research*, *89*(11), 977–982. https://doi.org/10.1161/hh2301.100982

Nystoriak, M. A., & Bhatnagar, A. (2018). Cardiovascular Effects and Benefits of Exercise. *Frontiers in Cardiovascular Medicine*, *5*, 135. https://doi.org/10.3389/fcvm.2018.00135

Prathima, S., & Asha Devi, S. (1999). Adaptations in lactate dehydrogenase and its isozymes in aging mammalian myocardium: Interaction of exercise and temperature. *Mechanisms of Ageing and Development*, *108*(1), 61–75. https://doi.org/10.1016/S0047-6374(99)00004-4

Rafalski, K., Abdourahman, A., & Edwards, J. G. (2007). Early Adaptations to Training: Upregulation of α-Myosin Heavy Chain Gene Expression. *Medicine & Science in Sports & Exercise*, *39*(1), 75–82. https://doi.org/10.1249/01.mss.0000240324.08406.3d

Rinne, P., Ahola-Olli, A., Nuutinen, S., Koskinen, E., Kaipio, K., Eerola, K., Juonala, M., Kähönen, M., Lehtimäki, T., Raitakari, O. T., & Savontaus, E. (2015). Deficiency in Melanocortin 1 Receptor Signaling Predisposes to Vascular Endothelial Dysfunction and Increased Arterial Stiffness in Mice and Humans. *Arteriosclerosis, Thrombosis, and Vascular Biology*, *35*(7), 1678–1686. https://doi.org/10.1161/ATVBAHA.114.305064

Rivera-Brown, A. M., & Frontera, W. R. (2012). Principles of Exercise Physiology: Responses to Acute Exercise and Long-term Adaptations to Training. *PM&R*, *4*(11), 797–804. https://doi.org/10.1016/j.pmrj.2012.10.007

Savarese, G., Division of Cardiology, Department of Medicine, Karolinska Insitutet, Stockholm, Sweden, Department of Cardiology, Karolinska University Hospital, Stockholm, Sweden, Lund, L. H., Division of Cardiology, Department of Medicine, Karolinska Insitutet, Stockholm, Sweden, & Department of Cardiology, Karolinska University Hospital, Stockholm, Sweden. (2017). Global Public Health Burden of Heart Failure. *Cardiac Failure Review*, *03*(01), 7. https://doi.org/10.15420/cfr.2016:25:2

Schiöth, H. B., Chhajlani, V., Muceniece, R., Klusa, V., & Wikberg, J. E. S. (1996). Major pharmacological distinction of the ACTH receptor from other melanocortin receptors. *Life Sciences*, *59*(10), 797–801. https://doi.org/10.1016/0024-3205(96)00370-0

Seo, D. Y., Kwak, H.-B., Kim, A. H., Park, S. H., Heo, J. W., Kim, H. K., Ko, J. R., Lee, S. J., Bang, H. S., Sim, J. W., Kim, M., & Han, J. (2020). Cardiac adaptation to exercise training in health and disease. *Pflügers Archiv - European Journal of Physiology*, *472*(2), 155–168. https://doi.org/10.1007/s00424-019-02266-3

Smith, A. I., & Funder, J. W. (1988). Proopiomelanocortin Processing in the Pituitary, Central Nervous System, and Peripheral Tissues. *Endocrine Reviews*, *9*(1), 159–179. https://doi.org/10.1210/edrv-9-1-159

Sohal, D. S., Nghiem, M., Crackower, M. A., Witt, S. A., Kimball, T. R., Tymitz, K. M., Penninger, J. M., & Molkentin, J. D. (2001). Temporally Regulated and Tissue-Specific Gene Manipulations in the Adult and Embryonic Heart Using a Tamoxifen-Inducible Cre Protein. *Circulation Research*, *89*(1), 20–25. https://doi.org/10.1161/hh1301.092687

Suominen, A., Rubio, G. S., Ruohonen, S., Szabó, Z., Pohjolainen, L., Ghimire, B., Ruohonen, S. T., Saukkonen, K., Ijas, J., Skarp, S., Kaikkonen, L., Cai, M., Wardlaw, S. L., Ruskoaho, H., Talman, V., Savontaus, E., Kerkelä, R., & Rinne, P. (2023). *α-Melanocyte-Stimulating Hormone Regulates Pathological Cardiac Remodeling by Activating Melanocortin 5 Receptor in Cardiomyocytes* [Preprint]. Physiology. https://doi.org/10.1101/2023.04.06.535956

Tamura, N., Ogawa, Y., Chusho, H., Nakamura, K., Nakao, K., Suda, M., Kasahara, M., Hashimoto, R., Katsuura, G., Mukoyama, M., Itoh, H., Saito, Y., Tanaka, I., Otani, H., Katsuki, M., & Nakao, K. (2000). Cardiac fibrosis in mice lacking brain natriuretic peptide. *Proceedings of the National Academy of Sciences*, *97*(8), 4239–4244. https://doi.org/10.1073/pnas.070371497

Thapa, K., Kadiri, J. J., Saukkonen, K., Pennanen, I., Ghimire, B., Cai, M., Savontaus, E., & Rinne, P. (2023). Melanocortin 1 receptor regulates cholesterol and bile acid metabolism in the liver. *eLife*, *12*, e84782. https://doi.org/10.7554/eLife.84782

Versteeg, D. H. G., Van Bergen, P., Adan, R. A. H., & De Wildt, D. J. (1998). Melanocortins and cardiovascular regulation. *European Journal of Pharmacology*, *360*(1), 1–14. https://doi.org/10.1016/S0014-2999(98)00615-3

Wang, Y., Wisloff, U., & Kemi, O. (2010). Animal models in the study of exercise-induced cardiac hypertrophy. *Physiological Research*, 633–644. https://doi.org/10.33549/physiolres.931928

Weiner, R. B., & Baggish, A. L. (2012). Exercise-Induced Cardiac Remodeling. *Progress in Cardiovascular Diseases*, *54*(5), 380–386. https://doi.org/10.1016/j.pcad.2012.01.006

Weiss, A., & Leinwand, L. A. (1996). THE MAMMALIAN MYOSIN HEAVY CHAIN GENE FAMILY. *Annual Review of Cell and Developmental Biology*, *12*(1), 417–439. https://doi.org/10.1146/annurev.cellbio.12.1.417

Wolf Horrell, E. M., Boulanger, M. C., & D'Orazio, J. A. (2016). Melanocortin 1 Receptor: Structure, Function, and Regulation. *Frontiers in Genetics*, *7*. https://doi.org/10.3389/fgene.2016.00095

Yamaoka-Tojo, M., Tojo, T., Shioi, T., Masuda, T., Inomata, T., & Izumi, T. (2006). Central Neurotranspeptide, Alpha-Melanocyte-Stimulating Hormone (.ALPHA.-MSH) is Upregulated in Patients with Congestive Heart Failure. *Internal Medicine*, *45*(7), 429–434. https://doi.org/10.2169/internalmedicine.45.1546

Yang, Y. (2011). Structure, function and regulation of the melanocortin receptors. *European Journal of Pharmacology*, *660*(1), 125–130. https://doi.org/10.1016/j.ejphar.2010.12.020